The Journal of Chemical Physics

Temperature expansions in the square-shoulder fluid. I. The Wiener–Hopf function

Cite as: J. Chem. Phys. **152**, 124112 (2020); https://doi.org/10.1063/1.5142661
Submitted: 16 December 2019 . Accepted: 09 March 2020 . Published Online: 27 March 2020

O. Coquand, and M. Sperl

AIP Publishing

The Journal of Chemical Physics ARTICLE scitation.org/journal/jcp

Temperature expansions in the square-shoulder fluid. I. The Wiener–Hopf function

Cite as: J. Chem. Phys. 152, 124112 (2020); doi: 10.1063/1.5142661
Submitted: 16 December 2019 • Accepted: 9 March 2020 •
Published Online: 27 March 2020

O. Coquand[1,a] and M. Sperl[1,2,b]

AFFILIATIONS

[1]Institut für Materialphysik im Weltraum, Deutsches Zentrum für Luft- und Raumfahrt (DLR), 51170 Köln, Germany
[2]Institut für Theoretische Physik, Universität zu Köln, 50937 Köln, Germany

[a]**Author to whom correspondence should be addressed:** oliver.coquand@dlr.de
[b]**Electronic mail:** matthias.sperl@dlr.de

ABSTRACT

We investigate the spatial structure of dense square-shoulder fluids. To this end, we derive analytical perturbative solutions of the Ornstein–Zernike equation in the low- and high-temperature limits as expansions around the known hard sphere solutions. We then discuss the suitability of perturbative approaches in relation to the Ornstein–Zernike equation. Our analytical expressions are shown to reproduce reasonably well numerical data in the appropriate regimes.

I. INTRODUCTION

The static structure factor is a function that characterizes the internal structure of a fluid. It is also directly accessible to experiments, notably via scattering methods. It carries quite a lot of information on the thermodynamic properties of the fluid[1]—it can be used to derive the equation of state—and at least part of the dynamics of arrest in the supercooled regime.[2–5]

However, from a theoretical point of view, computing a structure factor reveals to be particularly difficult and few analytical results have been established so far. One of the first systems where a structure factor was computed analytically is the hard-sphere system, where a first pathway has been designed by Wertheim and Thiele,[6–8] then followed by Baxter[9] who proposed an alternative method where the full complexity of the structure factor is captured by a remarkably simple function. These works have then triggered a series of studies to refine our understanding of the hard-sphere fluid's structure.[10–23]

One of the simplest generalizations of the hard-sphere potential is the square-shoulder potential, which consists of adding a finite region of constant positive potential outside of the hard-core. It shares most properties with the hard sphere potential: it is finite-range, fully repulsive, and prevents particles from getting too close to each other. Moreover, this potential has two natural hard-sphere limits: when the shoulder potential is very strong—or equivalently the temperature is very low, the outer-core becomes hard, and on the other hand, when it becomes very soft, or equivalently when the temperature is very high, only the hard inner-core plays a significant role. Despite these properties and a significant effort toward the theoretical understanding of this potential by the use of various methods, such as improved mean-spherical approximation,[24] thermodynamic perturbation theories,[25–27] and Rational Fraction Approximation (RFA),[28,29] no explicit analytical expression of the associated structure factor has been proposed yet, to the best of our knowledge. The closest result to such a solution has been gotten by the use of the Rational Fraction Approximation (RFA),[28,29] which, in the spirit of the first works on the hard-sphere system,[6–8] is based on truncations of functions in Laplace space. More precisely, one function related to the Laplace transform of the pair-correlation function $g(r)$ is expressed as a Padé approximant, the coefficients of which are then fixed by physical constraints. However, in the square-shoulder case, one of these constraint equations is transcendental and has to be solved numerically.

Our goal in this study is to get an understanding of how complexity emerges in this seemingly simple system by an investigation of the behavior of the structure factor of the square-shoulder fluid in the vicinity of its hard-sphere limits where its expression is known.

Starting from Baxter's solution,[9] which is the hard-sphere solution with the simplest formulation, we build the lowest order corrections to the hard-sphere behavior in a perturbative fashion, both in the low temperature limit where, compared to the particle's typical energy, the shoulder appears quasi-hard and in the high-temperature regime where the soft core potential barrier is small compared to their typical kinetic energy. This allows us to highlight how the structure of the Ornstein–Zernike equation prevents the construction of a simple solution in this latter regime, already at lowest order.

This paper is organized as follows: in Sec. II, we recall the method of Baxter. In Secs. III and IV, we build the low- and high-temperature expansions around that solution, respectively, and discuss the properties of the perturbative series. Finally, we compare our results to various sets of numerical data. The thermodynamic properties described by those structure factors are described in Paper II.[30]

II. REMINDER: THE HARD-SPHERE SYSTEM

First, we recall Baxter's derivation of the structure factor of the hard-sphere fluid.[9] The diameter of the hard spheres is called R. Remembering that in a fluid the structure factor, $S(q)$ has no singularity, the Wiener–Hopf factorization can be used to write it as follows:

$$S(q) = (Q(q)Q(-q))^{-1}. \tag{1}$$

Additionally, Q is a real function.[9] In an isotropic fluid, S does not depend on the direction of the wave vector q, and the Wiener–Hopf function Q is related to its direct space counterpart by the following relation:

$$Q(q) = 1 - 2\pi\rho \int_0^{+\infty} dr\, e^{iqr} Q(r), \tag{2}$$

where $\rho = N/V$ is the fluid's density, N is the number of particles, and V is the volume of the system.

Finally, the Ornstein–Zernike equations can be rewritten in terms of the Wiener–Hopf function $Q(r)$,[9]

$$\begin{aligned} rc(r) &= -Q'(r) + 2\pi\rho \int_r^{+\infty} ds\, Q'(s)Q(s-r), \\ rh(r) &= -Q'(r) + 2\pi\rho \int_0^{+\infty} ds\, (r-s)h(|r-s|)Q(s), \end{aligned} \tag{3}$$

where $c(r)$ is the fluid's direct correlation function, and h is related to the pair correlation function g by $h(r) = g(r) - 1$.

If the Ornstein–Zernike equation are closed by the use of the Percus–Yevick equation,

$$c(r) = (1 - e^{U(r)/k_BT})g(r), \tag{4}$$

where $U(r)$ is the particle pair potential, we also get $c(r) = 0$ as long as $r > R$. Then, Eq. (3) naturally leads to choose $Q(r) = 0$ in this region as well. As a result, all integrals in Eq. (3) evaluate on a finite domain.

Because hard particles cannot overlap, $h(r) = -1$ for $r \leqslant R$. We therefore need to compute $Q(r)$ only in a region, where $h(r)$ is known exactly, what greatly simplifies the search for a solution. Two successive derivatives can, indeed, be applied to the second equation in Eq. (3) to yield

$$Q^{(3)}(r) = 0, \tag{5}$$

that is, Q is a polynomial of degree 2 in r.

Finally, plugging this condition back into Eq. (3), with the additional requirement that Q is continuous at $r = R$, gives the final result

$$Q(r) = \frac{a_b}{2} r^2 + b_b r + c_b, \tag{6}$$

where the three coefficients can be written in terms of R and the packing fraction $\varphi = \pi\rho R^3/6$,

$$\begin{aligned} a_b &= \frac{1+2\varphi}{(1-\varphi)^2}, \\ b_b &= -\frac{3R\varphi}{2(1-\varphi)^2}, \\ c_b &= -\frac{R^2}{2(1-\varphi)}. \end{aligned} \tag{7}$$

The structure factor is then easily deduced from Eqs. (2) and (1). The greatest strength of this formalism is that a function $S(q)$ with an *a priori* very involved expression is completely expressed in terms of a simple polynomial of degree two with only two independent coefficients. Therefore, such a method appears to be a promising candidate to investigate small deviations from the hard-sphere potential. A similar study has been conducted previously on the square-well potential,[31] which is similar to the square-shoulder potential from this perspective.

III. LOW-TEMPERATURE EXPANSION

The square-shoulder potential is defined by the addition of a region of constant, positive potential U_0 to the hard-sphere case,

$$U(r) = \begin{cases} +\infty, & 0 \leqslant r < R \\ U_0, & R \leqslant r < d \\ 0, & d \leqslant r, \end{cases} \tag{8}$$

where $d = \lambda R$ is the outer-core diameter. The packing fraction of the outer core $\phi = \pi\rho d^3/6$ can also be defined. The square-shoulder potential is one of the simplest generalizations of the hard-sphere potential with one additional characteristic length scale. In particular, it shares the properties of being entirely repulsive and short-range.

In order to solve the Ornstein–Zernike equation (3) with the Percus–Yevick closure, Eq. (4), we need simplifications in the three regions of Eq. (8). By analogy with the hard-sphere case, we know that inside the hard-core $g(r) = 0$ and in the outside region where $U(r) = 0$, the direct correlation function $c(r)$ is also equal to zero. We will, thus, assume $Q(r) = 0$ for $r > d$ [it is a trivial solution of Eq. (3)]. However, inside the soft core, additional assumptions are needed.

In the low-temperature limit $U_0 \gg k_B T$, the contact value $g(R^+)$ is higher than in the corresponding hard-sphere system. Indeed, the hard-sphere contact value in the Percus–Yevick approximation is

$$g(R^+) = \frac{2+\varphi}{2(1-\varphi)^2}, \tag{9}$$

which gets bigger and bigger as φ approaches 1. As the temperature is decreased, the potential in Eq. (8) resembles the one for hard-spheres of diameter d, whose packing fraction is not φ, but $\phi = \lambda^3\varphi > \varphi$. Thus, this contact value can grow quite big but is always finite if we do not allow ϕ to grow bigger than 1.

Then, for larger values of r inside the shoulder, after a very sharp decrease, $g(r)$ saturates to a value that is all the more small that the temperature is small. This can be explained in the following way: if $U_0 \gg k_B T$, very few particles have the possibility to interpenetrate in the shoulder region. The expected form of $g(r)$ is then that of a low density gas, which saturates to the value of the average fraction p of particles that are able to cross the potential barrier.

Since the decrease in $g(r)$ is very sharp, the contact value contributes little to the integrals in the Ornstein–Zernike equations. For our purpose, we will, thus, approximate g in the following way:

$$g(r) = p, \quad R < r < d. \tag{10}$$

There can be various ways to define the constant p, but its precise form has little impact on the quantitative results. For the moment, we will, therefore, leave it unspecified. Since p is all the more small as T is small, we will use it as a small parameter for our expansion.[41]

Plugging Eq. (10) back into the Ornstein–Zernike equation (3), it is convenient to split the Wiener–Hopf function into four parts,

$$Q(r) = \begin{cases} Q_I(r), & 0 \leqslant r < d-R \\ Q_{II}(r), & d-R \leqslant r < R \\ Q_{III}(r), & R \leqslant r < d \\ 0, & r \geqslant d. \end{cases} \tag{11}$$

Then, Eq. (3) can be rewritten as

$$\begin{aligned} (p-1)r &= -Q'_{III}(r) + 2\pi\rho \int_0^d Q(s)(s-r)ds \\ &\quad + 2\pi\rho\, p \int_0^{r-R} Q_I(s)(r-s)ds, \\ -r &= -Q'_{II}(r) + 2\pi\rho \int_0^d Q(s)(s-r)ds, \\ -r &= -Q'_I(r) + 2\pi\rho \int_0^d Q(s)(s-r)ds \\ &\quad + 2\pi\rho\, p \int_{r+R}^d Q_{III}(s)(r-s)ds. \end{aligned} \tag{12}$$

Note that due to the additional integral terms in the first and last equations, the condition (5) only holds in the region II (for $r \in [d-R; R]$). Acting with two derivatives on these equations leads to the following set of coupled differential equations:

$$\begin{aligned} Q'''_{III}(r) &= 2\pi\rho\, p\big(Q_I(r+R) + R\,Q'_I(r+R)\big), \\ Q'''_I(r) &= -2\pi\rho\, p\big(Q_{III}(r-R) + R\,Q'_{III}(r-R)\big). \end{aligned} \tag{13}$$

As the left-hand side of these equations is proportional to the small parameter p, we can already anticipate that Q_I and Q_{III} can be written as a polynomial of degree two plus a small correction. Equations (13) can be solved exactly (the details are given in Appendix A).

The main results are as follows: both functions can be expressed as a function of six roots $\{X_i\}_{i\in[\![1;6]\!]}$, and generic coefficients $\{Y_i^I\}_{i\in[\![1;6]\!]}$ and $\{Y_i^{III}\}_{i\in[\![1;6]\!]}$ to be determined by the boundary conditions, in the following way:

$$Q_{III}(r) = \sum_{i=1}^{6} Y_i^{III}\, e^{X_i r}, \; Q_I(r) = \sum_{i=1}^{6} Y_i^I\, e^{X_i r}. \tag{14}$$

Equation (13) imposes the following relation:

$$\begin{cases} +\mathrm{i}Y_j^I - Y_j^{III} = 0, & j \leqslant 3, \\ -\mathrm{i}Y_j^I - Y_j^{III} = 0, & j \geqslant 4, \end{cases} \tag{15}$$

so that we can restrict ourselves to $\{Y_i^{III}\}_{i\in[\![1;6]\!]}$ that we will simply denote $\{Y_i\}_{i\in[\![1;6]\!]}$. Moreover, the Wiener–Hopf function Q must be real; therefore, for $i \leqslant 3$,

$$Y_i = Y_{i+3}^*, \tag{16}$$

which ensures that the number of constraints from the boundary conditions is sufficient to solve completely Eq. (13).

The roots X_i have the following behavior when p is small:

$$X_i \underset{p\to 0}{\sim} O(p^{1/3}) \tag{17}$$

so that the general solution [Eq. (14)] expanded at order $O(p)$ is a polynomial of degree 3 in r.

Finally, the Ornstein–Zernike equation (12) can be solved using the following ansatz:

$$Q_i(r) = e_i\frac{r^3}{6} + a_i\frac{r^2}{2} + b_i\, r + c_i, \tag{18}$$

where $i \in \{I, II, III\}$ and $e_{II} = 0$. For the sake of simplicity, let us decompose each coefficient according to its p expansion: $e_i = e_i^{(1)}p + O(p^2)$, $a_i = a^{(0)} + a_i^{(1)}p + O(p^2)$, $b_i = b^{(0)} + b_i^{(1)}p + O(p^2)$, and $c_i = c^{(0)} + c_i^{(1)}p + O(p^2)$. For each of these coefficients, the leading order term is independent of the considered region and is consistent with Baxter's solution for hard-spheres of diameter $d = \lambda R$,

$$\begin{aligned} a^{(0)} &= \frac{1+2\phi}{(1-\phi)^2}, \\ b^{(0)} &= -\frac{3d\phi}{2(1-\phi)^2}, \\ c^{(0)} &= -\frac{d^2}{2(1-\phi)}. \end{aligned} \tag{19}$$

The other coefficients are as follows:

$$
\begin{aligned}
e_I^{(1)} &= \frac{6\phi}{d(1-\phi)},\\
a_I^{(1)} &= \frac{\phi}{\lambda^4(1-\phi)^2}\left[\lambda^4(\phi-10)-27\phi+4\lambda(1+8\phi)\right],\\
b_I^{(1)} &= \frac{3R(\lambda-1)\phi}{2\lambda^3(1-\phi)^2}\left[1+\lambda+3\lambda^2+3\lambda^3+2(\lambda-5)\phi\right],\\
c_I^{(1)} &= \frac{R^2(\lambda-1)}{2\lambda^2(1-\phi)}\left[-3\phi+\lambda(\lambda+\lambda^2+\phi)\right],
\end{aligned}
\tag{20}
$$

$$
\begin{aligned}
a_{II}^{(1)} &= -\frac{\phi}{\lambda^4(1-\phi)^2}\left[27\phi+\lambda^4(4+5\phi)-4\lambda(1+8\phi)\right],\\
b_{II}^{(1)} &= \frac{3R\phi}{2\lambda^3(1-\phi)^2}\left[-1+\lambda^4+2(5-6\lambda+\lambda^4)\phi\right],\\
c_{II}^{(1)} &= \frac{R^2(\lambda^2-1)}{2\lambda^2(1-\phi)}\left[-3\phi+\lambda^2(1+2\phi)\right],
\end{aligned}
\tag{21}
$$

$$
\begin{aligned}
e_{III}^{(1)} &= -\frac{6\phi}{d(1-\phi)},\\
a_{III}^{(1)} &= -\frac{\phi\left[27\phi^2-4\lambda\phi(1+8\phi)+\lambda^4(1+2\phi+6\phi^2)\right]}{\lambda^4(1-\phi)^2},\\
b_{III}^{(1)} &= \frac{3R\phi\left[-1+2\lambda^2+\lambda^4+2\phi(5+\lambda(\lambda^3-\lambda-6))\right]}{2\lambda^3(1-\phi)^2},\\
c_{III}^{(1)} &= \frac{R^2}{2\lambda^2(1-\phi)}\left[\lambda^4+\phi\left(3+2\lambda(\lambda-2)(\lambda+1)^2\right)\right].
\end{aligned}
\tag{22}
$$

These terms are the first correction to the Wiener–Hopf function of hard-spheres, once a fraction of their hard-core becomes soft. Since the solution of the Ornstein–Zernike equation is exactly known, it is to be noted that such a computation is easily generalized to higher orders in p in which case the limiting assumption should be the form of $g(r)$, which is taken to be constant inside the integrals. It then appears that going to higher and higher orders in powers of p amounts to take as an ansatz for $Q(r)$ a piecewise polynomial of increasing degree.

IV. HIGH-TEMPERATURE EXPANSION

A. The full Percus–Yevick solution

We now turn to the high-temperature regime of the square-shoulder potential [Eq. (8)], $U_0 \ll k_BT$. Thanks to the Percus–Yevick closure [Eq. (4)], we already have sufficient knowledge inside the hard-core, and outside the potential range: as in the low-temperature case, we only need further an approximation inside the soft core $r \in [R; d]$. Since we are still dealing with a potential with only one additional length scale, it is convenient to use the splitting [Eq. (11)], so that the Ornstein–Zernike equation now reads

$$
\begin{aligned}
rh(r) &= -Q'_{III}(r) + 2\pi\rho\int_0^d Q(s)(s-r)ds\\
&\quad + 2\pi\rho\int_0^{r-R} Q_I(s)(r-s)g(|r-s|)ds,\\
-r &= -Q'_{II}(r) + 2\pi\rho\int_0^d Q(s)(s-r)ds,\\
-r &= -Q'_{I}(r) + 2\pi\rho\int_0^d Q(s)(s-r)ds\\
&\quad + 2\pi\rho\int_{r+R}^d Q_{III}(s)(r-s)g(|r-s|)ds.
\end{aligned}
\tag{23}
$$

In region II, the ansatz (6) still holds; for the two other regions, however, we need knowledge about the pair correlation function inside the shoulder. However, contrary to the low-temperature case, where the pair correlation function approaches a small constant, in the high-temperature regime, $g(r)$ approaches its hard sphere value outside the hard core—further corrections are of next order in an expansion in powers of $\Gamma = U_0/k_BT$—whose full exact analytical expression is not known, to the best of our knowledge. The problem of finding an expression of the hard-sphere pair-correlation function $g(r)$ within Percus–Yevick's approximation has nonetheless been solved explicitly by Wertheim in the region $r \in [R; 2R]$[6] and then used in a number of subsequent studies.[8,11,32–36]

For the sake of simplicity, we use here a different but equivalent approach: instead of giving an explicit expression to $g(r)$, the Percus–Yevick equation (4) combined with Eq. (3) can be used to re-express g as a function of Q alone. Equation (23) becomes non-linear in Q, but a careful splitting of each part of the Wiener–Hopf function in the Γ expansion, combined with the knowledge of the order $O(\Gamma^0)$, which is nothing but Baxter's solution [Eq. (6)], is sufficient to solve the equations. The details are given in Appendix B.

The main result is that Q_{III} can still be expressed in the following form:

$$
Q_{III} = \sum_{i=1}^{6} Y_i e^{X_i r},
\tag{24}
$$

where the X_i's are the roots of some specific polynomial. However, their high-temperature expansion has the following form:

$$
X_i = X_i^{(0)} + \Gamma X_i^{(1)} + O(\Gamma^2)
\tag{25}
$$

so that Q does not take a polynomial form anymore,

$$
Q_{III} = \sum_{i=1}^{6} Y_i e^{X_i^0 r}\left[1 + (X_i^1 r)\Gamma\right] + O(\Gamma^2).
\tag{26}
$$

Given the involved expressions of $X_i^{(0)}$'s, which are the roots of a polynomial of degree three, such an expression does not yield very useful analytical results when the boundary condition equations are solved. In the following, we design further approximation schemes so as to get a better analytical framework to deal with the high-temperature regime.

This form of Q's expansion should not come as a surprise in as much as the Ornstein–Zernike equations on the Wiener–Hopf function Q [Eq. (23)], depend explicitly on the pair correlation function

in a regime where its analytical expression is already quite heavy.[6] The fact that the Γ expansion of Q is not a polynomial, even at the lowest order is a hint that Baxter's solution does not yield a convenient starting point for an expansion at high temperature.

B. Approximations of the pair correlation function

In order to get a simpler approximation of $Q(r)$, the first ingredient we need is an analytical approximant of $g(r)$ inside the shoulder. As already stated, to the lowest order in Γ, we can restrict ourselves to an approximate expression of the hard-sphere $g(r)$ in the region near the hard-core in the Percus–Yevick approximation.

The Ornstein–Zernike equation (3) relates directly the pair correlation function to the Wiener–Hopf function. In the hard-sphere case, it is, thus, possible to use Baxter's solution [Eq. (6)] to get a polynomial approximant of $g(r)$ in the vicinity of the hard core. As a matter of fact, defining $F(r) = rh(r)$, Eq. (3) can be written as

$$F(R+\delta r) = 0 + 2\pi\rho \int_0^R Q_b(s)F(R+\delta r - s)ds. \tag{27}$$

Calling $F_n(r)$ the polynomial obtained by truncating the Taylor expansion of F at order $O(\delta r^n)$, we get an expression whose precision is typically of order $O(\delta^n)$, where $\delta = \lambda - 1$.

Such polynomial approximants are, however, ill-behaved and lead to unstable solutions except for very low values of δ. Indeed, even if they reproduce well the behavior of F near the core, high order terms lead very rapidly to excessive, positive or negative, values of F (and thus g) at odds with the expected physical tendency (see Fig. 1).

To overcome this difficulty, we chose to use the simplest exponential ansatz compatible with the two first orders of the δ expansion, namely,

$$F_{exp}(r) = F_0 \exp\left(\frac{F_1}{F_0}(r-R)\right), \tag{28}$$

with

$$F_0 = -\frac{R\varphi(-5+2\varphi)}{2(1-\varphi)^2}, \quad F_1 = -\frac{\varphi(10-2\varphi+\varphi^2)}{(1-\varphi)^3}. \tag{29}$$

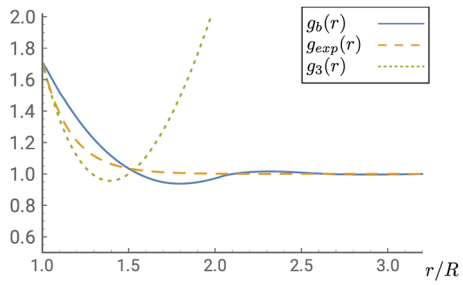

FIG. 1. Comparison between Baxter's pair correlation function g_b (solid line) and different truncations, for a hard-sphere system of packing fraction $\varphi = 0.2$. The dotted line corresponds to a truncation of Eq. (27) at order $O(\delta^3)$ and leads to very unphysical behavior. The dashed line corresponds to the exponential ansatz [Eq. (28)] used in the following.

The corresponding pair correlation function g_{exp} is displayed in Fig. 1. It approximates well Baxter's solution in the immediate vicinity of $r = R$ and far away from it. However, it misses the typical oscillatory behavior. Clearly, the quality of such an ansatz is diminished by going to higher values of δ, especially if φ is also quite high, but its precision cannot be captured by a simple power of δ, it is not anymore a small-shell expansion.

Obviously, better approximations of g can be designed—recall that its exact expression within the Percus–Yevick approximation is known for $\delta \leqslant 2$[6]—but we want here only to work out the simplest, yet physical, solution for the square-shoulder structure factor in a high-temperature expansion around Baxter's solution. As we show in the following, even this simplified solution is quite involved.

C. The truncated Percus–Yevick solution

As a consequence of the truncations of $g(r)$, we cannot work with the first equation of (23), since the terms of order $O(\Gamma^0)$ do not cancel anymore and Q_{III} is of order $O(\Gamma)$. Instead, the Percus–Yevick equation should be used to determine Q_{III}. In the appropriate region, it reads

$$\begin{aligned}(1-e^{\Gamma})(F(r)+r) &= rc(r) \\ &= -Q'_{III}(r) + 2\pi\rho\int_r^d Q'_{III}(s)Q_b(s-r)ds + O(\Gamma^2),\end{aligned} \tag{30}$$

where we have used the fact that since Q_{III} should go to zero as $\Gamma \to 0$—this is the hard-sphere high-temperature limit—the second factor in the integral can be replaced by its hard-sphere value Q_b.

The natural way to proceed is then to take derivatives to get a linear differential equation,

$$\Gamma F'' = Q'''_{III} + 2\pi\rho\left(c_b Q''_{III} + b_b Q'_{III} + a_b Q_{III}\right). \tag{31}$$

Note that such an expression is possible, thanks to the polynomial characteristic of Q_b. A simple solution ansatz can be found, with the form of F,

$$Q(r) = q_0\left(e^{q_1(r-d)} - 1\right), \tag{32}$$

but it can be shown not to fulfill the boundary conditions of Eq. (30) before derivation. Therefore, a solution of the homogeneous equation of the following form:

$$Q_H(r) = q_0 + q_1 e^{x_1 r} + q_2 e^{x_2 r} + q_3 e^{x_3 r}, \tag{33}$$

where $\{x_i\}$ are the roots of

$$X^3 + 2\pi\rho\left(c_b X^2 + b_b X + a_b\right) \tag{34}$$

must be added.

We recover the same problem as in the full Percus–Yevick case: the general solution is expressed in terms of exponential terms, not reducible into polynomials by a simple Γ expansion. This impedes the expression of the coefficients in Q as simple functions of the boundary conditions. Therefore, we must push our approximation even further.

In order to do so, note that if δ is not too big, the hard-sphere term in the convolution integral in Eq. (30) is not too different from

its constant term. We can, thus, safely replace Q_b by c_b. We then do not need to take derivatives to find a linear differential equation. The general solution for Q_{III} has the following form:

$$Q_{III}(r) = q_0\, e^{q_1 r} + q_2\, e^{q_3 r} + b_{III} r + c_{III}, \tag{35}$$

where $q_3 = 6\frac{\varphi}{R(1-\varphi)}$ comes from the homogeneous solution and $q_1 = F_1/F_0$ comes from the left-hand side term. The full expressions of the remaining coefficients can be found in Appendix C. As expected, Q_{III} is of order $O(\Gamma)$.

The remaining parts of the Wiener–Hopf function are then derived by plugging back into Eq. (23) the truncated expression of $g(r)$ and expression (35). As discussed before, Q_{II} still has a polynomial expression,

$$Q_{II}(r) = \frac{a_{II}}{2} r^2 + b_{II} r + c_{II}, \tag{36}$$

but Q_I and Q_{III} are not polynomial anymore,

$$Q_I(r) = g_I \frac{r^4}{24} + e_I \frac{r^3}{6} + a_I \frac{r^2}{2} + b_I\, r + c_I + q_{10}\, e^{q_1 r} + q_{11}\, e^{-q_1 r} + q_{30}\, e^{q_3 r}. \tag{37}$$

The quite lengthy expression of the coefficients is given in Appendix C. They illustrate the complexity of the solution, even at this level of approximation. As expected, both Q_I and Q_{II} can be written as $Q_b + O(\Gamma)$.

D. Discussion

The evolution of the Wiener–Hopf function Q with r is represented in Fig. 2. In particular, this graph displays how we get from the first hard-sphere limit to the high-temperature $Q(r)$, then to the low-temperature one, and finally to the second hard-sphere limit as the temperature is decreased. The shape of the square-shoulder $Q(r)$ appears to be quite similar to the hard-sphere one, except for a cusp located at $r = R$, which is associated with $g(r)$ developing a second discontinuity, as is well-known from previous data (see Refs. 25 and 28, for example).

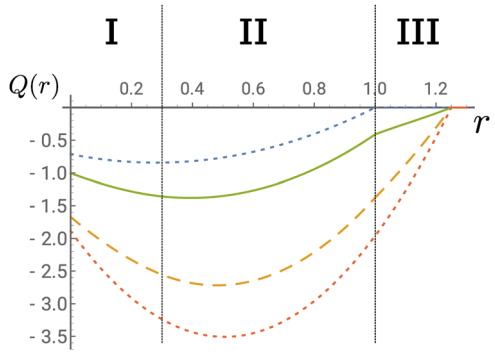

FIG. 2. Evolution of the Wiener–Hopf function $Q(r)$ for $\varphi = 0.3$ and $R = 1$. The dotted lines correspond to the two hard-sphere limits. The dashed line corresponds to the low-temperature expansion of Q for $\lambda = 1.25$ and $p = 0.8$. The solid line corresponds to the high-temperature expansion of Q for $\lambda = 1.25$ and $\Gamma = 1.2$. The values of the temperature parameters are chosen a bit outside of the range of applicability of our formulas to emphasize the deformations induced by temperature. In particular, due to the exponential behavior of p with T, quite large values must be taken to separate the low-temperature curve from its hard-sphere limit.

Note that, to the contrary, the transition for Q_I to Q_{II} remains smooth. Indeed, in Eq. (23), as $r \to d - R$ in region I, the last integral term in the Ornstein–Zernike equation smoothly goes to zero. Thus, the values of Q_I' and Q_{II}' become equal in that region.

All in all, we have investigated the possible constructions of high-temperature expansions around Baxter's hard-sphere solution, valid for square-shoulder systems with very weak shoulder potentials. It has been shown that the design of such an expansion turns out to be much more involved than in the low-temperature case. Even at the lowest level of approximation, the main asset of Baxter's solution, simplicity, is lost, along with the polynomial characteristic of the Wiener–Hopf function. The source of these difficulties has been identified: in the high-temperature case, the knowledge of the form of the hard-sphere pair correlation function outside of the core plays a crucial role but cannot be accurately captured by simple functions of the packing fraction φ. This will have further implications, as discussed in Paper II.[30]

V. NUMERICAL ACCURACY

In Sec. V, the results of our expansions are compared to various sets of numerical data.

A. The Wiener–Hopf function

The Wiener–Hopf function Q is mostly used in a theoretical context; hence, it is generally not computed in numerical investigations of structure problems. However, in Ref. 37, the author used a square-shoulder structure factor that was determined by numerically solving the $Q(r)$ version of the Ornstein–Zernike equation (3) within the Percus–Yevick approximation. The results are presented in Fig. 3. The numerical and analytical curves are almost on top of each other for each value of the parameters. This validates the numerical accuracy of our ansatz.

It is also instructive to look at the behavior of the analytical ansatz out of their range of applicability. For example, in Fig. 4, we represented the low-temperature ansatz for a dimensionless temperature $T = 2$. A striking feature is that the cusp at $r = R$ is barely visible, as we already discussed in Fig. 2. This can be related to the fact that in this framework, we supposed that $g(r) = p$ inside the shoulder, which is not a good approximation anymore when the temperature rises. As a result, the contact value $g(R^+)$, which is related to the slope difference on both sides of the cusp, is very much underestimated so that the cusp is less pronounced than on the numerical result without temperature expansions.

To the contrary, in the case of the high-temperature expansion, the cusp is overestimated at high values of Γ (see Fig. 5). As a matter of fact, the contact value $g(R^+)$ is now a linear function of Γ, which can, thus, become really wrong when Γ is large [see Ref. 30 for the full expression of $g(R^+)$ at high temperature]. Interestingly, as shown in Fig. 5, the form of the cusp gets better when the packing fraction increases: the $\Gamma \to 0$ limit of the contact value $g(R^+)$ is given by its hard sphere expression (9), which increases with φ. Therefore, for higher packing fractions, the overestimation of the Γ correction to the contact value at lower temperatures is comparatively weaker, hence a better numerical agreement.

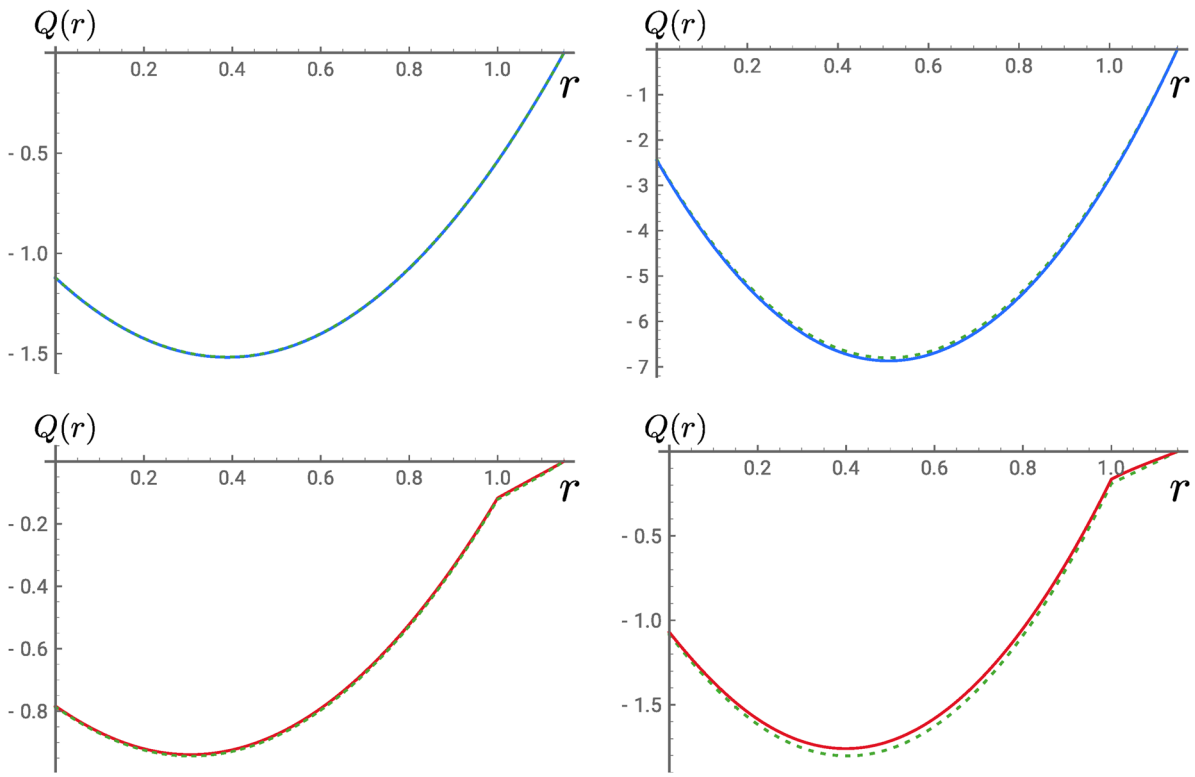

FIG. 3. Comparison of our expansions with the numerical solution of Eq. (3) used in Ref. 37 for $\lambda = 1.15$. The solid line corresponds to the analytical result; the dashed one corresponds to the numerical data. The top panels display the low-temperature ansatz for $\Gamma = 7.5$, and the bottom panels display the high-temperature ansatz for $\Gamma = 0.5$. In the left column, $\varphi = 0.27$; in the right column, $\varphi = 0.48$.

B. Structure factor

As a next step, we compare the structure factors built from our expansions to more realistic data. Indeed, it is known that the Percus–Yevick closure, despite its analytical simplicity, leads to thermodynamical inconsistencies, for example. A much better closure, from the point of view of numerical accuracy, is the Rogers–Young closure,[38] which is built explicitly to be thermodynamically consistent. It also compares very well to numerical simulations. Thus, we can expect that results from the Rogers–Young closure are more accurate than ours and use them to get an estimation of how good the Percus–Yevick approximation is in such a system in typical ranges of parameters. The comparison is displayed in Fig. 6.

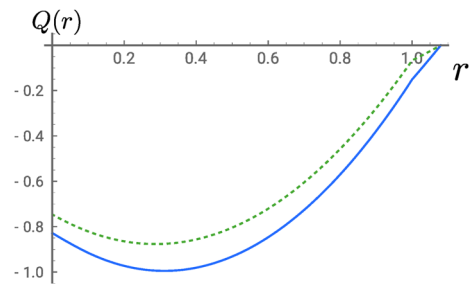

FIG. 4. Evolution of $Q(r)$ for $\lambda = 1.08$, $\Gamma = 0.5$, and $\varphi = 0.27$. The solid line corresponds to the low-temperature result; the dashed line corresponds to the numerical solution.

For low enough packing fractions, the agreement between the results from the two closures is good, but it deteriorates when the fluid gets denser. More precisely, as can be seen in the case of the high-temperature expansion, it is the first peak of the structure factor that carries the biggest error, which means that our structure factors tend to overestimate the enforcement of localization of the particles in the fluid. Let us stress, though, that on this dataset, $\Gamma = 0.5$, which is already quite large for a $\Gamma \ll 1$ expansion.

The case of the low-temperature expansion requires a closer look. Indeed, the agreement with the Rogers–Young data for $\varphi = 0.48$ is quite poor, what could come as a surprise since the low-temperature expansion is, as we saw before, much better behaved than its high-temperature counterpart. In order to understand a bit better this result, it is necessary to recall that in the low-temperature case, the reference point for the expansion is a hard-sphere system with packing fraction $\phi = \varphi \lambda^3$. Therefore, not only φ but also λ is a crucial quantity. In particular, for $\varphi = 0.48$ and $\lambda = 1.15$, as shown

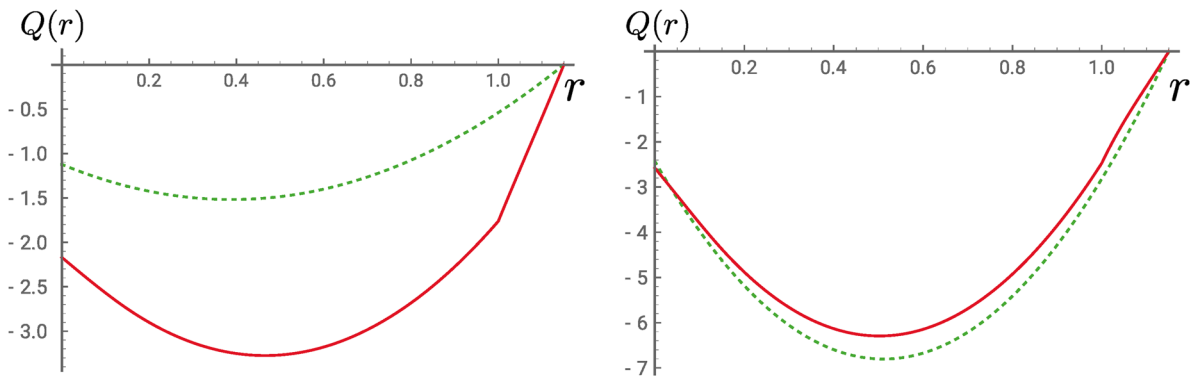

FIG. 5. Evolution of $Q(r)$ for $\lambda = 1.15$, $\Gamma = 7.5$, and $\varphi = 0.27$ (left) or $\varphi = 0.48$ (right). The solid line corresponds to the high-temperature result; the dashed line corresponds to the numerical solution.

on this example, the outer-core packing fraction is $\phi \simeq 0.73$ so that the reference system can hardly be considered as being in its fluid state. It is to be expected that even in the hard-sphere case, the structure factor determination is not very precise at such high packing fractions. Extra caution is therefore needed in the low-temperature case to ensure that the reference state used in the expansion is a well-defined one. As a final illustration, it is shown in Fig. 7 that even when λ is only lowered to 1.12—in which case $\phi \simeq 0.67$—the agreement between our Percus–Yevick results and the Rogers–Young structure factor is much better.

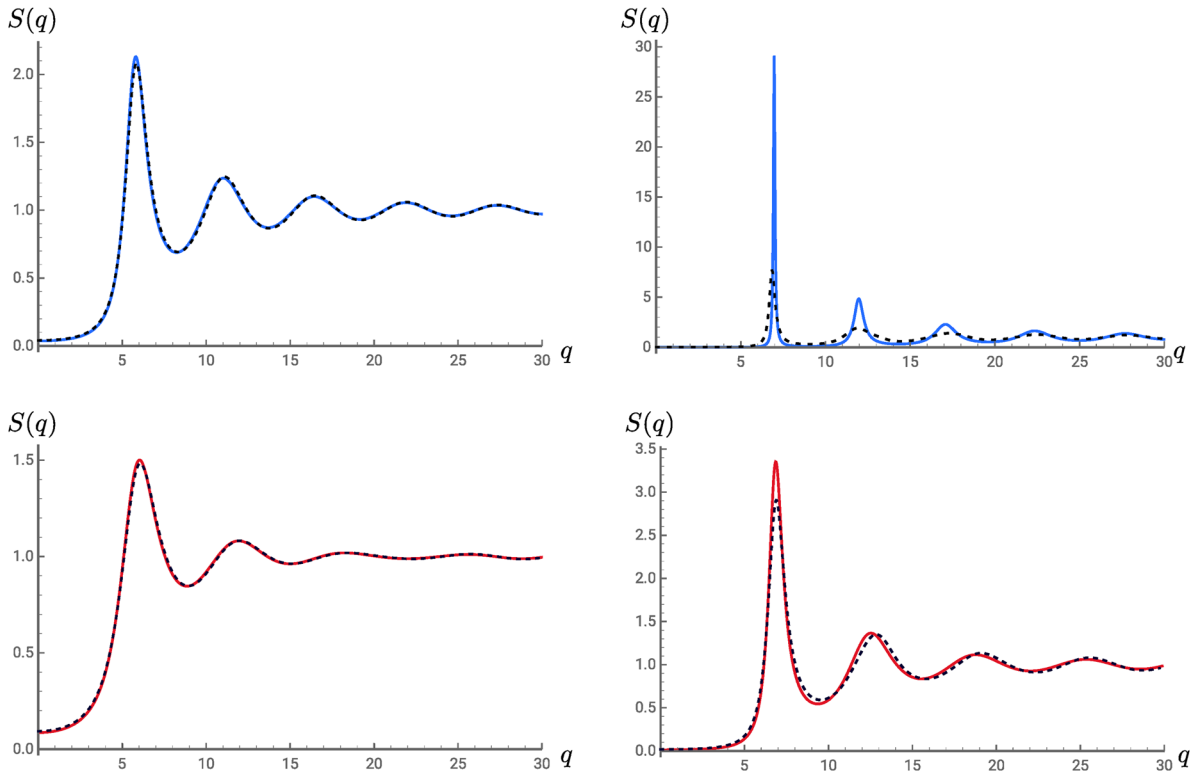

FIG. 6. Comparison of our expansions with the numerical solution of the Ornstein–Zernike equation with the Rogers–Young closure for $\lambda = 1.15$. The solid line corresponds to the analytical result; the dashed one corresponds to the numerical data. The top panels display the low-temperature ansatz for $\Gamma = 7.5$, and the bottom panels display the high-temperature ansatz for $\Gamma = 0.5$. In the left column, $\varphi = 0.27$; in the right column, $\varphi = 0.48$.

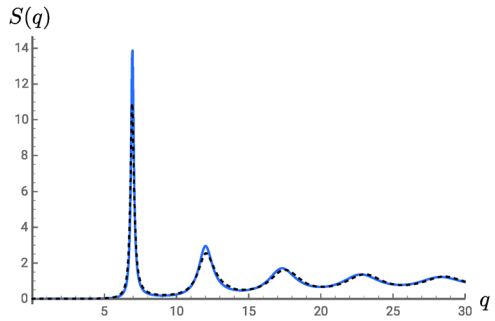

FIG. 7. Evolution of $S(q)$ for $\lambda = 1.12$, $\Gamma = 7.5$, and $\varphi = 0.48$. The solid line corresponds to the low-temperature result; the dashed line corresponds to the numerical solution.

C. Pair correlation function

Finally, we compare our results to those obtained by the rational fraction approximation by Yuste *et al.*,[28,29] which are the closest to a fully analytical solution without expansions. However, in their work, they represented the pair correlation function—which was shown to compare well to numerical data from various simulations[25,39,40]—which in our setup requires an additional Fourier transform. This causes some numerical artifacts in the vicinity of the discontinuities of g where very large wave number data are required. The comparison is shown in Fig. 8.

Let us first stress that the data presented in Refs. 28 and 29 are mostly in the range where the temperature is neither small nor large so that our expansions are not expected to be very precise. Second, following the same line of argument as the one used in Sec. V B, we chose not to represent the results for low-temperature expansion since for so big values of λ, the outer-core packing fraction is too large for the hard-sphere $T \to 0$ limit to be properly defined. With that in mind, the agreement between the high-temperature Percus–Yevick solution and the rational fraction approximation and simulation data appears to be surprisingly satisfactory. This can be used to validate the additional set of approximations we used in order to derive fully analytical expressions in the high-temperature limit.

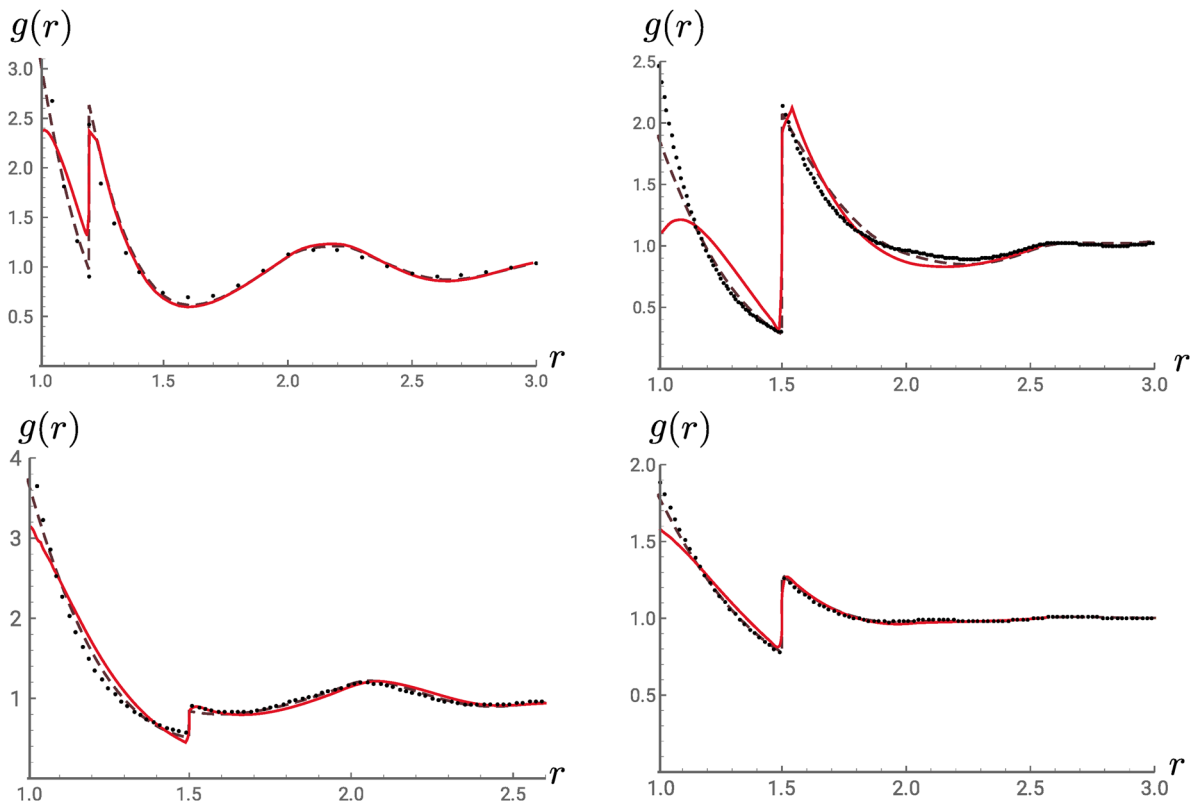

FIG. 8. Pair correlation functions. The dashed line corresponds to the rational fraction approximation ansatz from Refs. 28 and 29, dots correspond to results from various simulations,[25,39,40] and the solid line corresponds to the high-temperature expansion. The top-left graph is for $\lambda = 1.2$, $T = 1$, and $\varphi = 0.4$; the top-right graph is for $\lambda = 1.5$, $T = 0.5$, and $\varphi = 0.2094$; the bottom-left graph is for $\lambda = 1.5$, $T = 2$, and $\varphi = 0.4189$; and the bottom-right graph is for $\lambda = 1.5$, $T = 2$, and $\varphi = 0.2094$.

VI. CONCLUSION

All in all, we have shown how Baxter's solution to hard-sphere's structure factor can be extended to treat the high- and low-temperature sectors of the square-shoulder structure factor. In the low-temperature regime, our computation can be generalized to higher orders to improve precision. Moreover, the typical exponential dependence of p with respect to Γ generally ensures that already at moderate temperature, the low-temperature predictions should be quite good. However, at high temperatures, the lack of simple approximant of the hard-sphere pair correlation function outside of the core makes Baxter's solution a not so judicious starting point for a temperature expansion. This result has two main origins: first, the Percus–Yevick closure is particularly adapted to the hard-sphere potential—it reduces the problem to the computation of $Q(r)$ in a region where $g(r)$ is known exactly—but this cannot be easily generalized to any other potential. Second, the Ornstein–Zernike equation involves a convolution integral that appears to be poorly adapted to the design of perturbative expansions other than the virial one (indeed, the convolution integral is proportional to the density). Finally, comparison with numerical data showed reasonable agreement.

ACKNOWLEDGMENTS

This work was funded by DAAD. The authors would like to thank T. Kranz for careful reading of this manuscript. We thank A. Santos and N. Gadjisade for providing the numerical data.

APPENDIX A: LOW TEMPERATURE EQUATIONS—EXACT SOLUTION

Let us first rewrite the Ornstein–Zernike equation (13) in the following form:

$$\begin{cases} \Psi_1^{(3)}(r) = A\,\Psi_2(r) + B\,\Psi_2'(r) \\ \Psi_2^{(3)}(r) = -A\,\Psi_1(r) - B\,\Psi_1'(r), \end{cases} \tag{A1}$$

where $\Psi_1(r) = Q_{III}(r)$, $\Psi_2(r) = Q_I(r + R)$, $A = 12p\varphi/R^3$, and $B = 12p\varphi/R$. Both Ψ_1 and Ψ_2 are solutions of the following equation:

$$y^{(6)} + B^2 y'' + 2AB y' + A^2 y = 0, \tag{A2}$$

whose characteristic polynomial is

$$X^6 + B^2X^2 + 2AB\,X + A^2 = \big(X^3 + \mathrm{i}(BX + A)\big)\big(X^3 - \mathrm{i}(BX + A)\big), \tag{A3}$$

and its roots are, thus, known. The general solution is a combination of exponentials of the six roots, which can be divided into three sets of complex conjugates $\{X_1^{\pm}, X_2^{\pm}, X_3^{\pm}\}$, with the additional condition that it is a real function (what imposes conditions on the relative coefficients of the exponentials of two conjugate roots). Explicitly, these roots are given by

$$\begin{cases} X_1^{\pm} = \dfrac{1}{3(f_{\mp})^{1/3}}\left[\mp\mathrm{i}\dfrac{12(p\varphi)}{R^2}\,3^{2/3} + 3^{1/3}(f_{\mp})^{2/3}\right] \\ X_2^{\pm} = \dfrac{\pm\mathrm{i}}{6(f_{\mp})^{1/3}}\left[(\pm\sqrt{3}\mathrm{i} + 1)\dfrac{12(p\varphi)}{R^2}\,3^{1/6}\sqrt{3}\right. \\ \qquad \left. + 3^{1/3}(\pm\mathrm{i} + \sqrt{3})(f_{\mp})^{2/3}\right] \\ X_3^{\pm} = \dfrac{1}{6(f_{\mp})^{1/3}}\left[(\sqrt{3} \pm \mathrm{i})\dfrac{12(p\varphi)}{R^2}\,3^{1/6}\sqrt{3}\right. \\ \qquad \left. - 3^{1/3}(-1 \mp \mathrm{i}\sqrt{3})(f_{\mp})^{2/3}\right], \end{cases} \tag{A4}$$

where

$$\begin{aligned} \frac{R^3}{18p} \times f_{\pm} &= \pm 3\mathrm{i}\varphi + \sqrt{\pm\mathrm{i}\varphi^2(\pm 9\mathrm{i} + 16p\varphi)} \\ &\underset{p\to 0}{=} p\varphi^2\left[-\frac{8}{3} \pm \mathrm{i}\frac{32}{27}(p\varphi) + \frac{256}{243}(p\varphi)^2\right] + O(p^4). \end{aligned} \tag{A5}$$

The polynomial in Eq. (A3) can only be canceled if one if its factors is zero. The only difference between those factors is the change of a "+" sign into a "−" in the second factor. In the equations Eq. (A4) and Eq. (A5) above, the "±" signs are attributed to the roots of the first and second factor accordingly.

It must not be forgotten that although this solution is exact, the equation we used in the beginning [Eq. (A1)] is only meaningful in the low-temperature regime where the approximation that $g(r)$ is constant in the outer-core is justified; it should not be understood in any way as an exact solution to the Wiener–Hopf function problem in the presence of a full square shoulder potential.

We shall now derive the form of the general solution to Eq. (A1) at order $O(p)$. The low-temperature expansion of Eq. (A4) yields

$$\begin{cases} X_1^{\pm} \underset{p\to 0}{=} \pm\mathrm{i}\,\dfrac{2(p\varphi)^{1/3}}{R}\left(\dfrac{3}{2}\right)^{1/3} \\ \qquad \mp \dfrac{2(p\varphi)^{2/3}}{R}\left(\dfrac{2}{3}\right)^{1/3} + O(p^{4/3}) \\ X_2^{\pm} \underset{p\to 0}{=} \left(\dfrac{\sqrt{3} \pm \mathrm{i}}{2}\right)\dfrac{2(p\varphi)^{1/3}}{R}\left(\dfrac{3}{2}\right)^{1/3} \\ \qquad + \left(\dfrac{1 \pm \sqrt{3}\mathrm{i}}{2}\right)\dfrac{2(p\varphi)^{2/3}}{R}\left(\dfrac{2}{3}\right)^{1/3} + O(p^{4/3}) \\ X_3^{\pm} \underset{p\to 0}{=} \left(\dfrac{-\sqrt{3} \mp \mathrm{i}}{2}\right)\dfrac{2(p\varphi)^{1/3}}{R}\left(\dfrac{3}{2}\right)^{1/3} \\ \qquad + \left(\dfrac{-1 \mp \sqrt{3}\mathrm{i}}{2}\right)\dfrac{2(p\varphi)^{2/3}}{R}\left(\dfrac{2}{3}\right)^{1/3} + O(p^{4/3}). \end{cases} \tag{A6}$$

As can be anticipated from the form of the characteristic polynomial Eq. (A3), it is expressed in terms of the sixth root of (−1) and (+1).

We now go back to the Wiener–Hopf function. Let us define $X_4 = X_1^-$, $X_5 = X_2^-$, $X_6 = X_3^-$, and the following coefficients:

$$Q_{III}(r) = \sum_{i=1}^{6} Y_i^{III}\,e^{X_i r},\quad Q_I(r) = \sum_{i=1}^{6} Y_i^{I}\,e^{X_i r}. \tag{A7}$$

The Ornstein–Zernike equation (13) imposes

$$\begin{cases} +\mathrm{i}Y_j^I - Y_j^{III} = 0, & j \leqslant 3 \\ -\mathrm{i}Y_j^I - Y_j^{III} = 0, & j \geqslant 4, \end{cases} \tag{A8}$$

In the following, we will, thus, only work with the set $\{Y_j^{III}\}$ that we will simply denote $\{Y_j\}$.

Moreover, the Wiener–Hopf function must be real; therefore,

$$Y_i = Y_{i+3}^*. \tag{A9}$$

Then, we introduce some more adapted notations,

$$\alpha_j = Y_j + Y_j^*, \ \gamma_j = \mathrm{i}(Y_j - Y_j^*), \tag{A10}$$

$$\xi_1 = \frac{2(\varphi)^{1/3}}{R}\left(\frac{3}{2}\right)^{1/3}, \ \xi_2 = \frac{2(\varphi)^{2/3}}{R}\left(\frac{2}{3}\right)^{1/3}, \tag{A11}$$

as a function of which the general solution of Eq. (13) can be expanded in powers of p,

$$\begin{cases} Q_I(r) \underset{p\to 0}{=} (\gamma_1+\gamma_2+\gamma_3) - \dfrac{p^{1/3}}{2}\Big(\xi_1(2\alpha_1+\alpha_2+\alpha_3) \\ \quad + \xi_1\sqrt{3}(\gamma_3-\gamma_2) + p^{1/3}\xi_2\sqrt{3}(\alpha_2+\alpha_3) \\ \quad + p^{1/3}\xi_2(2\gamma_1-\gamma_2+\gamma_3)\Big)r \\ \quad + \dfrac{p^{2/3}}{4}\xi_1\Big(\xi_1(\gamma_2+\gamma_3-2\gamma_1) + \sqrt{3}\xi_1(\alpha_3-\alpha_2) \\ \quad + 4\xi_2 p^{1/3}(\alpha_1-\alpha_2+\alpha_3)\Big)r^2 \\ \quad + (\xi_1)^3\dfrac{p}{6}(\alpha_1-\alpha_2-\alpha_3)r^3 + O(p^{4/3}), \\ Q_{III}(r) \underset{p\to 0}{=} (\alpha_1+\alpha_2+\alpha_3) + \dfrac{p^{1/3}}{2}(\xi_1(2\gamma_1+\gamma_2+\gamma_3) \\ \quad + \xi_1\sqrt{3}(\alpha_2-\alpha_3) + p^{1/3}\xi_2\sqrt{3}(\gamma_2+\gamma_3) \\ \quad + p^{1/3}\xi_2(\alpha_2-\alpha_3-2\alpha_1)\Big)r \\ \quad + \dfrac{p^{2/3}}{4}\xi_1\Big(\xi_1(\alpha_2+\alpha_3-2\alpha_1) + \sqrt{3}\xi_1(\gamma_2-\gamma_3) \\ \quad - 4\xi_2 p^{1/3}(\gamma_1-\gamma_2+\gamma_3)\Big)r^2 \\ \quad + (\xi_1)^3\dfrac{p}{6}(\gamma_2+\gamma_3-\gamma_1)r^3 + O(p^{4/3}). \end{cases} \tag{A12}$$

All in all, even if the general solution to the Ornstein–Zernike equation within our set of approximations is a sum of exponential functions, polynomial expressions for the Wiener–Hopf function are recovered in the frame of the p-expansion. Interestingly, Q_I and Q_{III}, when developed at order $O(p)$, see their degree simply be augmented by 1.

Finally, the general solution to the equation at the first order in p can be expressed as a degree three polynomial, what justifies the ansatz Eq. (18). Moreover, Eq. (A12) specifies the p dependence of such coefficients when retrieved in an expansion of the exponential solution. Plugging it back into the Ornstein–Zernike equation (12), we see that in the boundary condition equation, only the constant term should be taken into account in the integral terms with a p prefactor (the coefficients of higher order terms all vanish in the $p \to 0$ limit and are, thus, subdominant at this order). Only then should we plug back the ansatz Eq. (18) and express the boundary conditions in powers of p.

APPENDIX B: HIGH TEMPERATURE—THE FULL PERCUS-YEVICK SOLUTION

A first way to tackle the problem is to use the Percus–Yevick equation inside the soft core,

$$c(r) = \left(1 - e^{\Gamma}\right)g(r), \tag{B1}$$

combined with the Ornstein–Zernike equation for the direct correlation function,

$$rc(r) = -Q'(r) + \frac{12\varphi}{R}\int_r^d Q'(s)Q(s-r)ds. \tag{B2}$$

Plugging this back into Eq. (23) to replace every occurrence of $g(r)$ yields the following three equations:

- $r \in [R; d]$:

$$\begin{aligned} -r = &+\left(\frac{e^{\Gamma}}{1-e^{\Gamma}}\right)Q'_{III}(r) + \frac{12\varphi}{R^3}\int_0^d Q(s)(s-r)ds \\ &- \frac{12\varphi}{R^3(1-e^{\Gamma})}\int_0^{r-R} Q_I(s)Q'_{III}(r-s)ds \\ &+ \left(\frac{12\varphi}{R^3}\right)^2\frac{1}{1-e^{\Gamma}}\int_0^{r-R} Q_I(s) \\ &\times \int_{r-s}^d du\, Q'_{III}(u)Q_I(u-r+s)ds. \end{aligned} \tag{B3}$$

- $r \in [d-R; R]$:

$$-r = -Q'_{II}(r) + \frac{12\varphi}{R^3}\int_0^d Q(s)(s-r)ds. \tag{B4}$$

- $r \in [0; d-R]$:

$$\begin{aligned} -r = &-Q'_I(r) + \frac{12\varphi}{R^3}\int_0^d Q(s)(s-r)ds \\ &- \frac{12\varphi}{R^3(1-e^{\Gamma})}\int_{r+R}^d Q_{III}(s)Q'_{III}(r-s)ds \\ &+ \left(\frac{12\varphi}{R^3}\right)^2\frac{1}{1-e^{\Gamma}}\int_{r+R}^d Q_{III}(s) \\ &\times \int_{s-r}^d du\, Q'_{III}(u)Q_I(u-r+s)ds. \end{aligned} \tag{B5}$$

Equation (B4) still has the usual solution,

$$Q_{II}(r) = a_{II}\frac{r^2}{2} + b_{II}\,r + c_{II}. \tag{B6}$$

For the two remaining equations, we must explicitly use the Γ expansion. In the limit $\Gamma \to 0$, the solutions are

$$Q_{III}(r) \underset{\Gamma\to 0}{=} O(\Gamma), \quad Q_I(r) \underset{\Gamma\to 0}{=} Q_b(r) + O(\Gamma). \tag{B7}$$

A main difference between Eqs. (B5) and (B3), on the one hand, and the low-temperature equation (13), on the other hand, is the highly non-linear characteristic of the former. As a consequence, in order to get linear differential equations on the Wiener–Hopf function, we must not take two, but five additional derivatives. With the following notations:

$$v_0(\Gamma) = \frac{1}{1-e^{-\Gamma}} \geqslant 0\ ,\ v_1(\Gamma) = \frac{1}{e^{\Gamma}-1} \geqslant 0, \tag{B8}$$

$$\mathcal{A} = \frac{12\varphi}{R^3} > 0, \tag{B9}$$

$$\omega_0 = -\mathcal{A}\int_0^d s\,Q(s)ds \geqslant 0, \quad \omega_1 = -\mathcal{A}\int_0^d Q(s)ds, \tag{B10}$$

Eq. (B3) becomes

$$\begin{aligned} 0 = &-v_0\,Q_{III}^{(6)} + \mathcal{A}\,v_1\left(c_b\,Q_{III}^{(5)} + b_b\,Q_{III}^{(4)} + a_b\,Q_{III}^{(3)}\right) \\ &+ \mathcal{A}^2 v_1\Big[c_b^2\,Q_{III}^{(4)} + b_b^2\,Q_{III}'' + a_b^2\,Q_{III} \\ &+ 2a_b b_b\,Q_{III}' + 2a_b c_b\,Q_{III}'' + 2b_b c_b\,Q_{III}^{(3)}\Big] + O(\Gamma^2). \end{aligned} \tag{B11}$$

It is a linear differential equation, whose characteristic polynomial is

$$-v_0\,X^6 + v_1\,P_b(X)\,X^3 + v_1\,P_b(X)^2, \tag{B12}$$

where we defined

$$P_b(X) = \mathcal{A}\left(c_b\,X^2 + b_b\,X + a_b\right). \tag{B13}$$

Defining $v = v_0/v_1$, its roots can be found. Indeed, for arbitrary θ, the roots of

$$-v\mathcal{X}^2 + \theta\mathcal{X} + \theta^2 \tag{B14}$$

are

$$\mathcal{X}_\pm = \frac{\theta}{2v}\left[1 \pm \sqrt{1+4v}\right] = \theta\,\zeta_\pm \tag{B15}$$

so that, finally,

$$-vX^6 + P_b(X)\,X^3 + P_b(X)^2 = -v\left(X^3 - \zeta_+\,P_b(X)\right)\left(X^3 - \zeta_-\,P_b(X)\right). \tag{B16}$$

The remaining roots of polynomials of order three can then be found exactly. They all have the following form:

$$X_i = X_i^0 + \Gamma\,X_i^1 + O(\Gamma^2), \tag{B17}$$

with $X_i^0 \neq 0$ and $X_i^1 \neq 0$. The Q_{III} function, thus, expands as

$$Q_{III}(r) = \sum_{i=1}^{6} Y_i e^{X_i r} = \sum_{i=1}^{6} Y_i e^{X_i^0 r}\left(1 + (X_i^1 r)\Gamma\right) + O(\Gamma^2). \tag{B18}$$

Finally, the structure of the Γ expansion is not compatible with a polynomial Wiener–Hopf function. This is due to the fact that $X_i^0 \neq 0$, which is in strong contrast to what happened in the low-temperature expansion.

APPENDIX C: HIGH TEMPERATURE COEFFICIENTS

- Q_{III} coefficients:

  Let us recall the general form of Q_{III},

  $$Q_{III}(r) = q_0\,e^{q_1 r} + q_2\,e^{q_3 r} + b_{III}r + c_{III}.$$

  The exponents in the exponential terms are

  $$q_1 = -\frac{2(\varphi^2 - 2\varphi + 10)}{R(2\varphi^2 - 7\varphi + 5)}, \quad q_3 = \frac{6\varphi}{R(1-\varphi)}. \tag{C1}$$

  The coefficients q_0 and q_2 vanish, as expected, in the infinite temperature limit ($\Gamma \to 0$),

  $$q_0 = \Gamma\,\frac{R^2(5-2\varphi)^2\varphi}{4(5\varphi^3 - 18\varphi^2 + 3\varphi + 10)}\,e^{\frac{2(\varphi^2-2\varphi+10)}{2\varphi^2-7\varphi+5}}, \tag{C2}$$

  $$q_2 = \Gamma\,\frac{R^2\left((\varphi-1)^2(5\varphi^2 - 13\varphi - 10)((6\lambda-1)\varphi+1)e^{\frac{2\lambda(\varphi^2-2\varphi+10)+4\varphi}{2\varphi^2-7\varphi+5}} - 9(5-2\varphi)^2\varphi^3 e^{\frac{2(\varphi^2+10)}{2\varphi^2-7\varphi+5}}\right)}{36\varphi^2(5\varphi^3 - 18\varphi^2 + 3\varphi + 10)}\exp\left(-\frac{\lambda(-10\varphi^2 + 26\varphi + 20) + 4\varphi}{2\varphi^2 - 7\varphi + 5}\right). \tag{C3}$$

  Finally, the polynomial part of Q_{III} is parameterized by

  $$b_{III} = \Gamma\,\frac{R(1-\varphi)}{6\varphi}, \quad c_{III} = \Gamma\,\frac{R^2(1-\varphi)^2}{36\varphi^2}, \tag{C4}$$

  and also vanish at high temperatures.
- Q_{II} coefficients:

They are written as $a_{II} = a_b + a_{II}^{(1)}\,\Gamma$, $b_{II} = b_b + b_{II}^{(1)}\,\Gamma$, and $c_{II} = c_b + c_{II}^{(1)}\,\Gamma$, where a_b, b_b, and c_b are Baxter's values for the corresponding hard sphere system given by Eq. (7). The first order coefficients are given below,

$$
\begin{aligned}
a_{II}^{(1)} = {} & \frac{e^{-\frac{4(\varphi(3\varphi+2)+\lambda(\varphi^2-2\varphi+10))}{2\varphi^2-7\varphi+5}}}{3240(1-\varphi)^3\varphi^4(7\varphi-10)(\varphi^2-2\varphi+10)^4(5\varphi^2-13\varphi-10)} \\
& \times \Bigg(3645\, e^{\frac{8(2\varphi^2+5)}{2\varphi^2-7\varphi+5}} (5-2\varphi)^6 (40\varphi^5-224\varphi^4+397\varphi^3-139\varphi^2-460\varphi-100)\varphi^8 \\
& - 90\, e^{\frac{2(\varphi^2+17\varphi+10+\lambda(7\varphi^2-17\varphi+10))}{(\varphi-1)(2\varphi-5)}} (5-2\varphi)^2(\varphi^2-2\varphi+10)^4(13\varphi^6-1404\varphi^5+3693\varphi^4-2576\varphi^3-153\varphi^2+204\varphi-20)\varphi^3 \\
& + 90\, e^{\frac{2(7\varphi^2+2\varphi+10+\lambda(\varphi^2-2\varphi+10))}{(\varphi-1)(2\varphi-5)}} (5-2\varphi)^2(5\varphi^2-13\varphi-10)\Big((378\lambda^4+1260\lambda^3-3150\lambda^2+6726\lambda-20\,245)\varphi^{12} \\
& - 3(1062\lambda^4+4464\lambda^3-7170\lambda^2+20\,912\lambda-80\,567)\varphi^{11} + 6(3654\lambda^4+13\,428\lambda^3-26\,919\lambda^2+72\,236\lambda-222\,189)\varphi^{10} \\
& - 2(45\,090\lambda^4+168\,318\lambda^3-376\,596\lambda^2+928\,980\lambda-2\,125\,733)\varphi^9 \\
& + 9(33\,216\lambda^4+106\,008\lambda^3-295\,206\lambda^2+643\,148\lambda-964\,925)\varphi^8 \\
& - 18(37\,860\lambda^4+111\,984\lambda^3-360\,063\lambda^2+671\,954\lambda-641\,292)\varphi^7 \\
& + 3(385\,200\lambda^4+938\,880\lambda^3-3\,373\,668\lambda^2+5\,337\,048\lambda-3\,319\,589)\varphi^6 \\
& - 36(34\,500\lambda^4+72\,300\lambda^3-206\,655\lambda^2+226\,202\lambda-102\,809)\varphi^5 \\
& + 72(7500\lambda^4+25\,500\lambda^3-2925\lambda^2-44\,980\lambda+10\,191)\varphi^4 - 160(4500\lambda^3+9675\lambda^2-9870\lambda-4231)\varphi^3 \\
& + 1200(300\lambda^2+530\lambda-281)\varphi^2 - 6000(20\lambda+21)\varphi+20\,000\Big)\varphi^3 \\
& + 10\, e^{\frac{38\varphi+2\lambda(8\varphi^2-19\varphi+20)}{2\varphi^2-7\varphi+5}} (1-\varphi)^2((6\lambda-1)\varphi+1)(\varphi^2-2\varphi+10)^4 \\
& \times (65\varphi^8-7189\varphi^7+36\,587\varphi^6-46\,849\varphi^5-4207\varphi^4+28\,769\varphi^3-1222\varphi^2-1780\varphi+200) \\
& + e^{\frac{4(\varphi(3\varphi+2)+\lambda(\varphi^2-2\varphi+10))}{2\varphi^2-7\varphi+5}} (7\varphi^2-17\varphi+10)\Big(10(1620\lambda^6-1296\lambda^5-44\,550\lambda^4+200\,520\lambda^3-346\,770\lambda^2+443\,705)\varphi^{17} \\
& - 2(93\,960\lambda^6-62\,208\lambda^5-2\,871\,450\lambda^4+13\,671\,360\lambda^3-25\,718\,310\lambda^2+36\,425\,363)\varphi^{16} \\
& + 4(378\,270\lambda^6-227\,448\lambda^5-11\,209\,590\lambda^4+52\,126\,380\lambda^3-97\,114\,815\lambda^2+134\,693\,303)\varphi^{15} \\
& - 4(2\,046\,060\lambda^6-1\,031\,616\lambda^5-59\,803\,110\lambda^4+267\,733\,800\lambda^3-475\,849\,665\lambda^2+584\,842\,171)\varphi^{14} \\
& + 4(8\,495\,280\lambda^6-3\,522\,528\lambda^5-235\,477\,530\lambda^4+992\,313\,540\lambda^3-1\,633\,492\,575\lambda^2+1\,621\,901\,438)\varphi^{13} \\
& - 4(27\,138\,240\lambda^6-8\,118\,144\lambda^5-702\,588\,330\lambda^4+2\,711\,876\,940\lambda^3-3\,992\,650\,245\lambda^2+2\,909\,867\,434)\varphi^{12} \\
& + 10(26\,415\,072\lambda^6-3\,763\,584\lambda^5-623\,530\,224\lambda^4+2\,134\,579\,824\lambda^3-2\,691\,937\,350\lambda^2+1\,285\,613\,177)\varphi^{11} \\
& - 4(123\,444\,000\lambda^6+6\,905\,088\lambda^5-2\,495\,838\,420\lambda^4+7\,044\,079\,680\lambda^3-7\,024\,662\,225\lambda^2+1\,844\,967\,967)\varphi^{10} \\
& + 5(120\,528\,000\lambda^6+61\,585\,920\lambda^5-1\,961\,348\,256\lambda^4+3\,642\,478\,848\lambda^3-2\,081\,782\,296\lambda^2+247\,814\,725)\varphi^9 \\
& - 10(45\,360\,000\lambda^6+60\,134\,400\lambda^5-314\,960\,400\lambda^4-618\,929\,568\lambda^3+1\,194\,566\,364\lambda^2+184\,924\,679)\varphi^8 \\
& - 80(2\,025\,000\lambda^6-10\,692\,000\lambda^5-75\,168\,000\lambda^4+268\,399\,800\lambda^3-185\,576\,751\lambda^2-66\,979\,673)\varphi^7 \\
& + 400(810\,000\lambda^6-8\,626\,500\lambda^4+1\,634\,400\lambda^3+11\,216\,340\lambda^2-11\,624\,801)\varphi^6 \\
& - 320(1\,620\,000\lambda^5+1\,012\,500\lambda^4-12\,442\,500\lambda^3+2\,968\,875\lambda^2+531\,958)\varphi^5 \\
& + 8000(40\,500\lambda^4+36\,000\lambda^3-155\,925\lambda^2-55\,939)\varphi^4 - 20\,000(7200\lambda^3+5400\lambda^2+3991)\varphi^3 \\
& + 100\,000(360\lambda^2+553)\varphi^2+10\,000\,000\varphi-2\,000\,000\Big)\Bigg),
\end{aligned}
\tag{C5}
$$

$$
\begin{aligned}
b_{II}^{(1)} = {} & \frac{R\, e^{-\frac{4(3\varphi(\varphi+1)+\lambda(\varphi^2-2\varphi+10))}{2\varphi^2-7\varphi+5}}}{19\,440(\varphi-1)^3\varphi^5(7\varphi-10)(\varphi^2-2\varphi+10)^4(5\varphi^2-13\varphi-10)} \\
& \times \Big(10\,935(5-2\varphi)^6(55\varphi^5-323\varphi^4+643\varphi^3-406\varphi^2-505\varphi+50)\varphi^9\, e^{\frac{4(4\varphi^2+\varphi+10)}{2\varphi^2-7\varphi+5}} \\
& - 90(5-2\varphi)^2(\varphi^2-2\varphi+10)^4 e^{\frac{2(\varphi^2+19\varphi+10+\lambda(7\varphi^2-17\varphi+10))}{(\varphi-1)(2\varphi-5)}} \\
& \times (65\varphi^7-4817\varphi^6+13\,290\varphi^5-10\,843\varphi^4+1108\varphi^3+615\varphi^2-157\varphi+10)\varphi^3 \\
& + 90 e^{\frac{2(7\varphi^2+4\varphi+10+\lambda(\varphi^2-2\varphi+10))}{2\varphi^2-7\varphi+5}} (5-2\varphi)^2(5\varphi^2-13\varphi-10)\varphi^3 \\
& \times \Big(((1512\lambda^4+4788\lambda^3-13\,482\lambda^2+26\,070\lambda-84\,971)\varphi^{13} \\
& - 2(6561\lambda^4+26\,100\lambda^3-49\,824\lambda^2+121\,383\lambda-521\,728)\varphi^{12} \\
& + 6(15\,147\lambda^4+52\,758\lambda^3-123\,279\lambda^2+284\,553\lambda-991\,406)\varphi^{11} \\
& + (-382\,644\lambda^4-1\,335\,636\lambda^3+3\,511\,782\lambda^2-7\,558\,296\lambda+19\,824\,179)\varphi^{10} \\
& + 2(642\,978\lambda^4+1\,909\,386\lambda^3-6\,261\,489\lambda^2+12\,232\,674\lambda-21\,465\,637)\varphi^9 \\
& - 9(336\,096\lambda^4+900\,432\lambda^3-3\,495\,288\lambda^2+6\,027\,012\lambda-6\,914\,119)\varphi^8 \\
& + 6(883\,980\lambda^4+1\,900\,656\lambda^3-8\,714\,673\lambda^2+13\,149\,672\lambda-10\,213\,439)\varphi^7 \\
& - 3(2\,041\,200\lambda^4+3\,468\,240\lambda^3-15\,629\,724\lambda^2+18\,185\,940\lambda-11\,287\,201)\varphi^6 \\
& + 36(94\,500\lambda^4+198\,900\lambda^3-405\,165\lambda^2+17\,586\lambda-151\,624)\varphi^5 \\
& + (-540\,000\lambda^4-3\,168\,000\lambda^3-2\,329\,200\lambda^2+7\,987\,080\lambda+2\,474\,414)\varphi^4 \\
& + 20(18\,000\lambda^3+88\,200\lambda^2+14\,220\lambda-77\,689)\varphi^3 \\
& - 600(300\lambda^2+1080\lambda+259)\varphi^2+2000(30\lambda+59)\varphi-10\,000\Big) \\
& + 10 e^{\frac{42\varphi+2\lambda(8\varphi^2-19\varphi+20)}{2\varphi^2-7\varphi+5}} (1-\varphi)^2((6\lambda-1)\varphi+1)(\varphi^2-2\varphi+10)^4 \\
& \times (325\varphi^9-24\,930\varphi^8+128\,421\varphi^7-178\,815\varphi^6+13\,599\varphi^5+97\,101\varphi^4-19\,860\varphi^3-4059\varphi^2+1440\varphi-100) \\
& + e^{\frac{4(3\varphi(\varphi+1)+\lambda(\varphi^2-2\varphi+10))}{2\varphi^2-7\varphi+5}} (7\varphi^2-17\varphi+10) \\
& \times \Big(50(1296\lambda^6-1296\lambda^5-35\,802\lambda^4+164\,232\lambda^3-285\,534\lambda^2+387\,005)\varphi^{18} \\
& - 120(6399\lambda^6-5724\lambda^5-196\,128\lambda^4+951\,858\lambda^3-1\,797\,306\lambda^2+2\,718\,097)\varphi^{17} \\
& + 60(104\,004\lambda^6-88\,128\lambda^5-3\,102\,651\lambda^4+14\,761\,728\lambda^3-27\,668\,583\lambda^2+41\,544\,184)\varphi^{16} \\
& - 18(1\,902\,780\lambda^6-1\,474\,128\lambda^5-56\,018\,880\lambda^4+257\,529\,520\lambda^3-461\,962\,130\lambda^2+627\,546\,223)\varphi^{15} \\
& + 12(12\,009\,060\lambda^6-8\,498\,088\lambda^5-336\,540\,285\lambda^4+1\,464\,498\,360\lambda^3-2\,445\,166\,200\lambda^2+2\,770\,845\,353)\varphi^{14} \\
& - 12(39\,016\,080\lambda^6-24\,311\,664\lambda^5-1\,025\,133\,705\lambda^4+4\,121\,735\,040\lambda^3-6\,207\,195\,960\lambda^2+5\,444\,576\,974)\varphi^{13} \\
& + 3(388\,385\,280\lambda^6-198\,402\,048\lambda^5-9\,367\,176\,960\lambda^4+33\,886\,716\,960\lambda^3-44\,403\,756\,900\lambda^2+28\,162\,466\,203)\varphi^{12} \\
& - 12(186\,604\,560\lambda^6-69\,304\,896\lambda^5-3\,915\,970\,920\lambda^4+12\,058\,641\,720\lambda^3-12\,981\,156\,135\lambda^2+5\,646\,777\,676)\varphi^{11} \\
& + 3(968\,112\,000\lambda^6-74\,711\,808\lambda^5-16\,900\,935\,120\lambda^4+38\,689\,626\,240\lambda^3-29\,617\,889\,220\lambda^2+10\,006\,489\,853)\varphi^{10} \\
& - 5(483\,408\,000\lambda^6+198\,236\,160\lambda^5-4\,881\,731\,328\lambda^4+1\,378\,324\,800\lambda^3+5\,145\,650\,136\lambda^2+2\,052\,733\,129)\varphi^9 \\
& - 120(1\,620\,000\lambda^6-24\,537\,600\lambda^5-159\,615\,900\lambda^4+735\,475\,032\lambda^3-614\,923\,167\lambda^2-107\,477\,161)\varphi^8 \\
& + 60(24\,300\,000\lambda^6-16\,848\,000\lambda^5-320\,652\,000\lambda^4+488\,347\,200\lambda^3-96\,413\,184\lambda^2-224\,247\,415)\varphi^7 \\
& - 360(900\,000\lambda^6+3\,960\,000\lambda^5-7\,380\,000\lambda^4-28\,832\,000\lambda^3+13\,139\,800\lambda^2+340\,719)\varphi^6 \\
& + 480(540\,000\lambda^5+2\,193\,750\lambda^4-4\,185\,000\lambda^3-6\,452\,250\lambda^2-1\,956\,989)\varphi^5 \\
& - 12\,000(13\,500\lambda^4+45000\lambda^3-30600\lambda^2+8477)\varphi^4+120\,000(600\lambda^3+1275\lambda^2+1703)\varphi^3 \\
& - 1\,200\,000(15\lambda^2+2)\varphi^2-10\,500\,000\varphi+1\,000\,000)\Big), \qquad \text{(C6)}
\end{aligned}
$$

$$
\begin{aligned}
c_{II}^{(1)} = & -\frac{R^2}{19\,440(1-\varphi)^2\varphi^5(7\varphi-10)(\varphi^2-2\varphi+10)^4(5\varphi^2-13\varphi-10)}\, e^{-\frac{4(3\varphi(\varphi+1)+\lambda(\varphi^2-2\varphi+10))}{2\varphi^2-7\varphi+5}} \\
& \times \Bigg(32\,805\,(5-2\varphi)^6(5\varphi^4-28\varphi^3+54\varphi^2-35\varphi-50)\varphi^9 e^{\frac{4(4\varphi^2+\varphi+10)}{2\varphi^2-7\varphi+5}} \\
& - 90(5-2\varphi)^2(\varphi^2-2\varphi+10)^4(26\varphi^6-957\varphi^5+2550\varphi^4-2023\varphi^3+84\varphi^2+87\varphi-10)\varphi^3 e^{\frac{2(\varphi^2+19\varphi+10+\lambda(7\varphi^2-17\varphi+10))}{(\varphi-1)(2\varphi-5)}} \\
& + 90e^{\frac{2(7\varphi^2+4\varphi+10+\lambda(\varphi^2-2\varphi+10))}{(\varphi-1)(2\varphi-5)}}(5-2\varphi)^2(5\varphi^2-13\varphi-10)\varphi^3\big(2(189\lambda^4+504\lambda^3-2016\lambda^2+2946\lambda-12\,118)\varphi^{12} \\
& - 3(1062\lambda^4+3672\lambda^3-10\,362\lambda^2+16\,222\lambda-98\,039)\varphi^{11}+3(7308\lambda^4+21\,276\lambda^3-74\,682\lambda^2+119\,468\lambda-551\,639)\varphi^{10} \\
& - 4(22\,545\lambda^4+65\,475\lambda^3-257\,040\lambda^2+406\,503\lambda-1\,353\,716)\varphi^9 \\
& + 9(33\,216\lambda^4+77\,184\lambda^3-391\,584\lambda^2+608\,260\lambda-1\,273\,715)\varphi^8 \\
& - 18(37\,860\lambda^4+75\,672\lambda^3-471\,663\lambda^2+693\,514\lambda-896\,326)\varphi^7 \\
& + 3(385\,200\lambda^4+530\,640\lambda^3-4\,478\,364\lambda^2+6\,127\,116\lambda-5\,090\,155)\varphi^6 \\
& - 18(69\,000\lambda^4+55\,800\lambda^3-618\,630\lambda^2+652\,592\lambda-415\,987)\varphi^5 \\
& + 18(30\,000\lambda^4+36\,000\lambda^3-156\,600\lambda^2-77\,660\lambda-9553)\varphi^4 \\
& - 20(18\,000\lambda^3+25\,200\lambda^2-92\,580\lambda-13\,579)\varphi^3+600(300\lambda^2+380\lambda-451)\varphi^2-12\,000(5\lambda+4)\varphi+10\,000\big) \\
& + 10e^{\frac{42\varphi+2\lambda(8\varphi^2-19\varphi+20)}{2\varphi^2-7\varphi+5}}(1-\varphi)^2((6\lambda-1)\varphi+1)(\varphi^2-2\varphi+10)^4 \\
& \times(130\varphi^8-5123\varphi^7+24\,931\varphi^6-33\,695\varphi^5+1219\varphi^4+19\,573\varphi^3-2021\varphi^2-740\varphi+100) \\
& + e^{\frac{4(3\varphi(\varphi+1)+\lambda(\varphi^2-2\varphi+10))}{2\varphi^2-7\varphi+5}}(7\varphi^2-17\varphi+10)\big(20(810\lambda^6-1296\lambda^5-22\,680\lambda^4+109\,800\lambda^3-193\,680\lambda^2+301\,955)\varphi^{17} \\
& - 2(93\,960\lambda^6-143\,856\lambda^5-2\,926\,530\lambda^4+14\,999\,400\lambda^3-28\,746\,630\lambda^2+50\,793\,151)\varphi^{16} \\
& + 2(756\,540\lambda^6-1\,135\,296\lambda^5-22\,895\,460\lambda^4+115\,094\,160\lambda^3-218\,621\,970\lambda^2+387\,418\,181)\varphi^{15} \\
& - 20(409\,212\lambda^6-594\,216\lambda^5-12\,245\,580\lambda^4+59\,626\,872\lambda^3-108\,393\,921\lambda^2+175\,186\,735)\varphi^{14} \\
& + 20(1\,699\,056\lambda^6-2\,391\,120\lambda^5-48\,392\,073\lambda^4+223\,684\,020\lambda^3-378\,610\,254\lambda^2+514\,451\,747)\varphi^{13} \\
& - 20(5\,427\,648\lambda^6-7\,324\,992\lambda^5-145\,135\,152\lambda^4+622\,230\,840\lambda^3-950\,117\,175\lambda^2+1\,007\,708\,074)\varphi^{12} \\
& + (264\,150\,720\lambda^6-335\,798\,784\lambda^5-6\,492\,921\,120\lambda^4+25\,178\,139\,360\lambda^3-33\,450\,806\,700\lambda^2+25\,867\,546\,039)\varphi^{11} \\
& + (-493\,776\,000\lambda^6+578\,721\,024\lambda^5+10\,548\,668\,880\lambda^4-34\,996\,605\,120\lambda^3+38\,027\,120\,220\lambda^2-20\,070\,008\,909)\varphi^{10} \\
& + 5(120\,528\,000\lambda^6-113\,840\,640\lambda^5-2\,146\,782\,528\lambda^4+5\,287\,018\,176\lambda^3-3\,919\,962\,600\lambda^2+1\,401\,192\,947)\varphi^9 \\
& - 20(22\,680\,000\lambda^6-12\,182\,400\lambda^5-211\,296\,600\lambda^4-48\,778\,992\lambda^3+474\,553\,638\lambda^2-39\,460\,333)\varphi^8 \\
& - 20(8\,100\,000\lambda^6-31\,104\,000\lambda^5-266\,976\,000\lambda^4+1\,143\,273\,600\lambda^3-988\,064\,352\lambda^2+8\,993\,921)\varphi^7 \\
& + 40(8\,100\,000\lambda^6-9\,720\,000\lambda^5-88\,695\,000\lambda^4+111\,852\,000\lambda^3+12\,922\,200\lambda^2-51\,988\,453)\varphi^6 \\
& - 160(1\,620\,000\lambda^5-506\,250\lambda^4-18\,180\,000\lambda^3+8\,520\,750\lambda^2+561\,733)\varphi^5 \\
& + 8000(20\,250\lambda^4+4500\lambda^3-89\,775\lambda^2-41\,162)\varphi^4-40\,000(1800\lambda^3+675\lambda^2+1414)\varphi^3 \\
& + 100\,000(180\lambda^2+359)\varphi^2+3\,500\,000\varphi-\big)\Bigg).
\end{aligned}
\tag{C7}
$$

- Q_I coefficients:

  Q_I contains both a polynomial and an exponential part. We recall its form

$$
Q_I(r) = g_I\frac{r^4}{24}+e_I\frac{r^3}{6}+a_I\frac{r^2}{2}+b_I\,r+c_I+q_{10}\,e^{q_1 r}+q_{11}\,e^{-q_1 r}+q_{30}\,e^{q_3 r}.
$$

The coefficients q_1 and q_3 are inherited from Q_{III} and given above. Only the three coefficients present in the hard sphere solutions have a non-vanishing $\Gamma \to 0$ limit. They are written as $a_I = a_b + a_I^{(1)}\,\Gamma$, $b_I = b_b + b_I^{(1)}\,\Gamma$, and $c_I = c_b + c_I^{(1)}\,\Gamma$, where a_b, b_b, and c_b are Baxter's values for

the corresponding hard sphere system given by Eq. (7). The values of the first order corrections are as follows:

$$
\begin{aligned}
a_I^{(1)} = {} & \frac{e^{-\frac{4(\varphi(3\varphi+2)+\lambda(\varphi^2-2\varphi+10))}{2\varphi^2-7\varphi+5}}}{3240(1-\varphi)^3\varphi^4(7\varphi-10)(\varphi^2-2\varphi+10)^4(5\varphi^2-13\varphi-10)} \\
& \times \Bigg(3645\, e^{\frac{8(2\varphi^2+5)}{2\varphi^2-7\varphi+5}} (5-2\varphi)^6(40\varphi^5-224\varphi^4+397\varphi^3-139\varphi^2-460\varphi-100)\varphi^8 \\
& - 90\, e^{\frac{2(\varphi^2+17\varphi+10+\lambda(7\varphi^2-17\varphi+10))}{(\varphi-1)(2\varphi-5)}} (5-2\varphi)^2(\varphi^2-2\varphi+10)^4(13\varphi^6-1404\varphi^5+3693\varphi^4-2576\varphi^3-153\varphi^2+204\varphi-20)\varphi^3 \\
& + 90\, e^{\frac{2(7\varphi^2+2\varphi+10+\lambda(\varphi^2-2\varphi+10))}{(\varphi-1)(2\varphi-5)}} (5-2\varphi)^2(5\varphi^2-13\varphi-10)\big((378\lambda^4+1260\lambda^3-3150\lambda^2+6726\lambda-20\,119)\varphi^{12} \\
& - 3(1062\lambda^4+4464\lambda^3-7170\lambda^2+20\,912\lambda-80\,129)\varphi^{11} + 6(3654\lambda^4+13\,428\lambda^3-26\,919\lambda^2+72\,236\lambda-220\,596)\varphi^{10} \\
& - 4(22\,545\lambda^4+84\,159\lambda^3-188\,298\lambda^2+464\,490\lambda-1\,051\,432)\varphi^9 \\
& + 9(33\,216\lambda^4+106\,008\lambda^3-295\,206\lambda^2+643\,148\lambda-946\,361)\varphi^8 \\
& - 18(37\,860\lambda^4+111\,984\lambda^3-360\,063\lambda^2+671\,954\lambda-615\,930)\varphi^7 \\
& + 3(385\,200\lambda^4+938\,880\lambda^3-3\,373\,668\lambda^2+5\,337\,048\lambda-3\,006\,533)\varphi^6 \\
& - 36(34\,500\lambda^4+72\,300\lambda^3-206\,655\lambda^2+226\,202\lambda-63\,599)\varphi^5 \\
& + 72(7500\lambda^4+25\,500\lambda^3-2925\lambda^2-44\,980\lambda+29\,541)\varphi^4 \\
& - 80(9000\lambda^3+19\,350\lambda^2-19\,740\lambda+1213)\varphi^3 + 1200(300\lambda^2+530\lambda-131)\varphi^2 - 6000(20\lambda+21)\varphi+20\,000\big)\varphi^3 \\
& + 10\, e^{\frac{38\varphi+2\lambda(8\varphi^2-19\varphi+20)}{2\varphi^2-7\varphi+5}} (1-\varphi)^2((6\lambda-1)\varphi+1)(\varphi^2-2\varphi+10)^4 \\
& \times (65\varphi^8-7189\varphi^7+36\,587\varphi^6-46\,849\varphi^5-4207\varphi^4+28\,769\varphi^3-1222\varphi^2-1780\varphi+200) \\
& + e^{\frac{4(\varphi(3\varphi+2)+\lambda(\varphi^2-2\varphi+10))}{2\varphi^2-7\varphi+5}} (7\varphi^2-17\varphi+10)\big(10(1620\lambda^6-1296\lambda^5-44\,550\lambda^4+200\,520\lambda^3-345\,150\lambda^2+448\,475)\varphi^{17} \\
& - 2(93\,960\lambda^6-62\,208\lambda^5-2\,871\,450\lambda^4+13\,671\,360\lambda^3-25\,608\,150\lambda^2+36\,781\,223)\varphi^{16} \\
& + 4(378\,270\lambda^6-227\,448\lambda^5-11\,209\,590\lambda^4+52\,126\,380\lambda^3-96\,638\,535\lambda^2+136\,214\,483)\varphi^{15} \\
& - 4(2\,046\,060\lambda^6-1\,031\,616\lambda^5-59\,803\,110\lambda^4+267\,733\,800\lambda^3-473\,000\,085\lambda^2+593\,797\,486)\varphi^{14} \\
& + 4(8\,495\,280\lambda^6-3\,522\,528\lambda^5-235\,477\,530\lambda^4+992\,313\,540\lambda^3-1\,620\,526\,905\lambda^2+1\,661\,028\,218)\varphi^{13} \\
& - 4(27\,138\,240\lambda^6-8\,118\,144\lambda^5-702\,588\,330\lambda^4+2\,711\,876\,940\lambda^3-3\,946\,475\,385\lambda^2+3\,041\,213\,389)\varphi^{12} \\
& + 10(26\,415\,072\lambda^6-3\,763\,584\lambda^5-623\,530\,224\lambda^4+2\,134\,579\,824\lambda^3-2\,640\,413\,574\lambda^2+1\,421\,349\,431)\varphi^{11} \\
& - 4(123\,444\,000\lambda^6+6\,905\,088\lambda^5-2\,495\,838\,420\lambda^4+7\,044\,079\,680\lambda^3-6\,742\,004\,625\lambda^2+2\,510\,757\,187)\varphi^{10} \\
& + 5(120\,528\,000\lambda^6+61\,585\,920\lambda^5-1\,961\,348\,256\lambda^4+3\,642\,478\,848\lambda^3-1\,710\,913\,752\lambda^2+999\,963\,877)\varphi^9 \\
& - 10(45\,360\,000\lambda^6+60\,134\,400\lambda^5-314\,960\,400\lambda^4-618\,929\,568\lambda^3+1\,409\,831\,964\lambda^2+520\,834\,991)\varphi^8 \\
& - 80(2\,025\,000\lambda^6-10\,692\,000\lambda^5-75\,168\,000\lambda^4+268\,399\,800\lambda^3-202\,424\,751\lambda^2-78\,917\,885)\varphi^7 \\
& + 400(810\,000\lambda^6-8\,626\,500\lambda^4+1\,634\,400\lambda^3+11\,702\,340\lambda^2-8\,366\,171)\varphi^6 \\
& - 320(1\,620\,000\lambda^5+1\,012\,500\lambda^4-12\,442\,500\lambda^3+5\,500\,125\lambda^2+4\,354\,708)\varphi^5 \\
& + 8000(40\,500\lambda^4+36\,000\lambda^3-115\,425\lambda^2-30\,289)\varphi^4 \\
& - 20\,000(7200\lambda^3+5400\lambda^2-59)\varphi^3+100\,000(360\lambda^2+373)\varphi^2+10\,000\,000\varphi-2\,000\,000\big)\Bigg), \qquad \text{(C8)}
\end{aligned}
$$

$$
\begin{aligned}
b_I^{(1)} = {} & \frac{R\, e^{-\frac{4(3\varphi(\varphi+1)+\lambda(\varphi^2-2\varphi+10))}{2\varphi^2-7\varphi+5}}}{19\,440(\varphi-1)^3\varphi^5(7\varphi-10)(\varphi^2-2\varphi+10)^4(5\varphi^2-13\varphi-10)} \\
& \times \Bigg(10\,935\, e^{\frac{4(4\varphi^2+\varphi+10)}{2\varphi^2-7\varphi+5}} (5-2\varphi)^6(55\varphi^5-323\varphi^4+643\varphi^3-406\varphi^2-505\varphi+50)\varphi^9 \\
& - 90\, e^{\frac{2(\varphi^2+19\varphi+10+\lambda(7\varphi^2-17\varphi+10))}{(\varphi-1)(2\varphi-5)}} (5-2\varphi)^2(\varphi^2-2\varphi+10)^4
\end{aligned}
$$

$$
\begin{aligned}
&\times (65\varphi^7 - 4817\varphi^6 + 13\,290\varphi^5 - 10\,843\varphi^4 + 1108\varphi^3 + 615\varphi^2 - 157\varphi + 10)\varphi^3 \\
&+ 90\, e^{\frac{2(7\varphi^2+4\varphi+10+\lambda(\varphi^2-2\varphi+10))}{2\varphi^2-7\varphi+5}} (5-2\varphi)^2(5\varphi^2 - 13\varphi - 10)\big((1512\lambda^4 + 4788\lambda^3 - 13\,482\lambda^2 + 26\,826\lambda - 84\,089)\varphi^{13} \\
&- 2(6561\lambda^4 + 26\,100\lambda^3 - 49\,824\lambda^2 + 125\,325\lambda - 516\,499)\varphi^{12} \\
&+ 6(15\,147\lambda^4 + 52\,758\lambda^3 - 123\,279\lambda^2 + 294\,111\lambda - 979\,388)\varphi^{11} \\
&+ (-382\,644\lambda^4 - 1\,335\,636\lambda^3 + 3\,511\,782\lambda^2 - 7\,832\,724\lambda + 19\,486\,679)\varphi^{10} \\
&+ 2(642\,978\lambda^4 + 1\,909\,386\lambda^3 - 6\,261\,489\lambda^2 + 12\,733\,902\lambda - 20\,894\,452)\varphi^9 \\
&- 9(336\,096\lambda^4 + 900\,432\lambda^3 - 3\,495\,288\lambda^2 + 6\,331\,356\lambda - 6\,594\,541)\varphi^8 \\
&+ 6(883\,980\lambda^4 + 1\,900\,656\lambda^3 - 8\,714\,673\lambda^2 + 14\,088\,840\lambda - 9\,326\,291)\varphi^7 \\
&- 3(2\,041\,200\lambda^4 + 3\,468\,240\lambda^3 - 15\,629\,724\lambda^2 + 21\,009\,060\lambda - 8\,950\,585)\varphi^6 \\
&+ 36(94\,500\lambda^4 + 198\,900\lambda^3 - 405\,165\lambda^2 + 249\,786\lambda + 23\,486)\varphi^5 \\
&- 2(270\,000\lambda^4 + 1\,584\,000\lambda^3 + 1\,164\,600\lambda^2 - 1\,671\,540\lambda + 588\,893)\varphi^4 \\
&+ 20(18\,000\lambda^3 + 88\,200\lambda^2 + 68\,220\lambda - 16\,489)\varphi^3 - 600(300\lambda^2 + 1080\lambda + 559)\varphi^2 + 2000(30\lambda + 59)\varphi - 10\,000\big)\varphi^3 \\
&+ 10\, e^{\frac{42\varphi+2\lambda(8\varphi^2-19\varphi+20)}{2\varphi^2-7\varphi+5}} (1-\varphi)^2((6\lambda - 1)\varphi + 1)(\varphi^2 - 2\varphi + 10)^4 \\
&\times (325\varphi^9 - 24\,930\varphi^8 + 128\,421\varphi^7 - 178\,815\varphi^6 + 13\,599\varphi^5 + 97\,101\varphi^4 - 19\,860\varphi^3 - 4059\varphi^2 + 1440\varphi - 100) \\
&+ e^{\frac{4(3\varphi(\varphi+1)+\lambda(\varphi^2-2\varphi+10))}{2\varphi^2-7\varphi+5}} (7\varphi^2 - 17\varphi + 10) \\
&\times \big(50(1296\lambda^6 - 1296\lambda^5 - 35\,802\lambda^4 + 165\,528\lambda^3 - 285\,210\lambda^2 + 378\,887)\varphi^{18} \\
&- 60(12\,798\lambda^6 - 11\,448\lambda^5 - 392\,256\lambda^4 + 1\,918\,404\lambda^3 - 3\,590\,670\lambda^2 + 5\,328\,215)\varphi^{17} \\
&+ 60(104\,004\lambda^6 - 88\,128\lambda^5 - 3\,102\,651\lambda^4 + 14\,888\,736\lambda^3 - 27\,633\,159\lambda^2 + 40\,626\,490)\varphi^{16} \\
&- 18(1\,902\,780\lambda^6 - 1\,474\,128\lambda^5 - 56\,018\,880\lambda^4 + 260\,062\,480\lambda^3 - 461\,223\,050\lambda^2 + 610\,036\,803)\varphi^{15} \\
&+ 12(12\,009\,060\lambda^6 - 8\,498\,088\lambda^5 - 336\,540\,285\lambda^4 + 1\,481\,785\,920\lambda^3 - 2\,439\,894\,450\lambda^2 + 2\,661\,335\,948)\varphi^{14} \\
&- 12(39\,016\,080\lambda^6 - 24\,311\,664\lambda^5 - 1\,025\,133\,705\lambda^4 + 4\,183\,301\,520\lambda^3 - 6\,187\,482\,450\lambda^2 + 5\,101\,090\,309)\varphi^{13} \\
&+ 3(388\,385\,280\lambda^6 - 198\,402\,048\lambda^5 - 9\,367\,176\,960\lambda^4 + 34\,573\,700\,640\lambda^3 - 44\,170\,444\,500\lambda^2 + 24\,913\,174\,483)\varphi^{12} \\
&- 12(186\,604\,560\lambda^6 - 69\,304\,896\lambda^5 - 3\,915\,970\,920\lambda^4 + 12\,435\,518\,520\lambda^3 - 12\,844\,000\,455\lambda^2 + 4\,232\,182\,486)\varphi^{11} \\
&+ 3(968\,112\,000\lambda^6 - 74\,711\,808\lambda^5 - 16\,900\,935\,120\lambda^4 + 41\,162\,083\,200\lambda^3 - 28\,622\,898\,180\lambda^2 + 3\,256\,488\,773)\varphi^{10} \\
&- 5(483\,408\,000\lambda^6 + 198\,236\,160\lambda^5 - 4\,881\,731\,328\lambda^4 + 3\,100\,449\,600\lambda^3 + 5\,947\,049\,880\lambda^2 - 647\,233\,895)\varphi^9 \\
&- 120(1\,620\,000\lambda^6 - 24\,537\,600\lambda^5 - 159\,615\,900\lambda^4 + 690\,547\,032\lambda^3 - 644\,093\,967\lambda^2 - 110\,042\,995)\varphi^8 \\
&+ 60(24\,300\,000\lambda^6 - 16\,848\,000\lambda^5 - 320\,652\,000\lambda^4 + 501\,307\,200\lambda^3 - 115\,637\,184\lambda^2 - 349\,863\,331)\varphi^7 \\
&- 360(900\,000\lambda^6 + 3\,960\,000\lambda^5 - 7\,380\,000\lambda^4 - 19\,832\,000\lambda^3 + 15\,929\,800\lambda^2 - 10\,078\,081)\varphi^6 \\
&+ 480(540\,000\lambda^5 + 2\,193\,750\lambda^4 - 1\,485\,000\lambda^3 - 4\,089\,750\lambda^2 - 1\,680\,989)\varphi^5 \\
&- 12\,000(13\,500\lambda^4 + 45\,000\lambda^3 - 3600\lambda^2 + 18\,827)\varphi^4 \\
&+ 120\,000(600\lambda^3 + 1275\lambda^2 + 878)\varphi^3 - 1\,200\,000(15\lambda^2 - 13)\varphi^2 - 10\,500\,000\varphi + 1\,000\,000)\big),
\end{aligned}
\tag{C9}
$$

$$
\begin{aligned}
c_I^{(1)} = &- \frac{R^2\, e^{-\frac{4(3\varphi(\varphi+1)+\lambda(\varphi^2-2\varphi+10))}{2\varphi^2-7\varphi+5}}}{19\,440(1-\varphi)^2\varphi^5(7\varphi - 10)(\varphi^2 - 2\varphi + 10)^4(5\varphi^2 - 13\varphi - 10)} \\
&\times \Big(32\,805\, e^{\frac{4(4\varphi^2+\varphi+10)}{2\varphi^2-7\varphi+5}} (5-2\varphi)^6(5\varphi^4 - 28\varphi^3 + 54\varphi^2 - 35\varphi - 50)\varphi^9 \\
&- 90\, e^{\frac{2(\varphi^2+19\varphi+10+\lambda(7\varphi^2-17\varphi+10))}{(\varphi-1)(2\varphi-5)}} (5-2\varphi)^2(\varphi^2 - 2\varphi + 10)^4(26\varphi^6 - 957\varphi^5 + 2550\varphi^4 - 2023\varphi^3 + 84\varphi^2 + 87\varphi - 10)\varphi^3 \\
&+ 90\, e^{\frac{2(7\varphi^2+4\varphi+10+\lambda(\varphi^2-2\varphi+10))}{(\varphi-1)(2\varphi-5)}} (5-2\varphi)^2(5\varphi^2 - 13\varphi - 10)\big((378\lambda^4 + 1008\lambda^3 - 3654\lambda^2 + 6774\lambda - 24\,467)\varphi^{12}
\end{aligned}
$$

$$
\begin{aligned}
&- 6(531\lambda^4 + 1836\lambda^3 - 4587\lambda^2 + 9707\lambda - 49\,197)\varphi^{11} + 3(7308\lambda^4 + 21\,276\lambda^3 - 66\,312\lambda^2 + 140\,312\lambda - 555\,391)\varphi^{10}\\
&+ (-90\,180\lambda^4 - 261\,900\lambda^3 + 916\,056\lambda^2 - 1\,900\,980\lambda + 5\,486\,081)\varphi^9\\
&+ 18(16\,608\lambda^4 + 38\,592\lambda^3 - 174\,174\lambda^2 + 352\,319\lambda - 654\,915)\varphi^8\\
&- 9(75\,720\lambda^4 + 151\,344\lambda^3 - 834\,390\lambda^2 + 1\,610\,228\lambda - 1\,903\,537)\varphi^7\\
&+ 12(96\,300\lambda^4 + 132\,660\lambda^3 - 966\,501\lambda^2 + 1\,807\,953\lambda - 1\,438\,966)\varphi^6\\
&- 18(69\,000\lambda^4 + 55\,800\lambda^3 - 485\,430\lambda^2 + 857\,912\lambda - 540\,831)\varphi^5\\
&+ 72(7500\lambda^4 + 9000\lambda^3 - 14\,400\lambda^2 + 16\,810\lambda - 16\,577)\varphi^4 - 20(18\,000\lambda^3 + 52\,200\lambda^2 - 40\,380\lambda - 6769)\varphi^3\\
&+ 600(300\lambda^2 + 680\lambda - 111)\varphi^2 - 6000(10\lambda + 13)\varphi + 10\,000\big)\varphi^3\\
&+ 10\,e^{\frac{42\varphi+2\lambda(8\varphi^2-19\varphi+20)}{2\varphi^2-7\varphi+5}}(1-\varphi)^2((6\lambda-1)\varphi+1)(\varphi^2-2\varphi+10)^4\\
&\times(130\varphi^8 - 5123\varphi^7 + 24\,931\varphi^6 - 33\,695\varphi^5 + 1219\varphi^4 + 19\,573\varphi^3 - 2021\varphi^2 - 740\varphi + 100)\\
&+ e^{\frac{4(3\varphi(\varphi+1)+\lambda(\varphi^2-2\varphi+10))}{2\varphi^2-7\varphi+5}}(7\varphi^2 - 17\varphi + 10)\\
&\times\Big(10(1620\lambda^6 - 2592\lambda^5 - 42\,930\lambda^4 + 220\,680\lambda^3 - 401\,670\lambda^2 + 648\,175)\varphi^{17}\\
&- 4(46\,980\lambda^6 - 71\,928\lambda^5 - 1\,386\,720\lambda^4 + 7\,536\,420\lambda^3 - 14\,871\,330\lambda^2 + 27\,195\,773)\varphi^{16}\\
&+ 2(756\,540\lambda^6 - 1\,135\,296\lambda^5 - 21\,619\,710\lambda^4 + 115\,729\,200\lambda^3 - 226\,753\,020\lambda^2 + 416\,431\,751)\varphi^{15}\\
&- 20(409\,212\lambda^6 - 594\,216\lambda^5 - 11\,518\,281\lambda^4 + 60\,006\,816\lambda^3 - 112\,954\,005\lambda^2 + 190\,268\,218)\varphi^{14}\\
&+ 20(1\,699\,056\lambda^6 - 2\,391\,120\lambda^5 - 45\,229\,671\lambda^4 + 225\,412\,776\lambda^3 - 397\,526\,238\lambda^2 + 569\,568\,254)\varphi^{13}\\
&- 10(10\,855\,296\lambda^6 - 14\,649\,984\lambda^5 - 268\,890\,192\lambda^4 + 1\,256\,774\,976\lambda^3 - 2\,020\,017\,528\lambda^2 + 2\,305\,873\,787)\varphi^{12}\\
&+ (264\,150\,720\lambda^6 - 335\,798\,784\lambda^5 - 5\,933\,865\,600\lambda^4 + 25\,521\,631\,200\lambda^3 - 36\,325\,062\,540\lambda^2 + 31\,313\,237\,899)\varphi^{11}\\
&+ (-493\,776\,000\lambda^6 + 578\,721\,024\lambda^5 + 9\,411\,778\,800\lambda^4 - 35\,750\,358\,720\lambda^3 + 43\,142\,335\,020\lambda^2 - 26\,932\,888\,109)\varphi^{10}\\
&+ 5(120\,528\,000\lambda^6 - 113\,840\,640\lambda^5 - 1\,817\,857\,728\lambda^4 + 5\,534\,263\,872\lambda^3 - 5\,153\,367\,096\lambda^2 + 2\,365\,312\,889)\varphi^9\\
&- 20(22\,680\,000\lambda^6 - 12\,182\,400\lambda^5 - 132\,078\,600\lambda^4 + 22\,976\,208\lambda^3 + 279\,039\,294\lambda^2 - 32\,038\,459)\varphi^8\\
&- 160(1\,012\,500\lambda^6 - 3\,888\,000\lambda^5 - 36\,105\,750\lambda^4 + 137\,293\,200\lambda^3 - 130\,040\,019\lambda^2 + 18\,477\,964)\varphi^7\\
&+ 40(8\,100\,000\lambda^6 - 9\,720\,000\lambda^5 - 70\,470\,000\lambda^4 + 115\,092\,000\lambda^3 - 58\,708\,800\lambda^2 - 15\,808\,057)\varphi^6\\
&- 160(1\,620\,000\lambda^5 + 2\,531\,250\lambda^4 - 14\,805\,000\lambda^3 + 3\,492\,000\lambda^2 - 307\,817)\varphi^5\\
&+ 16\,000(10\,125\lambda^4 + 15\,750\lambda^3 - 33\,075\lambda^2 - 19\,201)\varphi^4 - 20\,000(3600\lambda^3 + 4050\lambda^2 + 3863)\varphi^3\\
&+ 200\,000(90\lambda^2 + 97)\varphi^2 + 6\,500\,000\varphi - 1\,000\,000\big)\Big).
\end{aligned}
\tag{C10}
$$

The other coefficients are

$$
g_I = \Gamma\,\frac{2(\varphi-1)}{R^2}, \quad e_I = -\Gamma\,\frac{(\varphi-1)^2}{3R\varphi},
\tag{C11}
$$

$$
q_{10} = \Gamma\,\frac{3R^2(5-2\varphi)^4\varphi^2(6\varphi^4 - 29\varphi^3 + 72\varphi^2 - 72\varphi + 50)}{16(\varphi^2-2\varphi+10)^3(5\varphi^3 - 18\varphi^2 + 3\varphi + 10)},
\tag{C12}
$$

$$
\begin{aligned}
q_{11} = \Gamma\,&\frac{3R^2(5-2\varphi)^4\varphi^2}{16(\varphi-1)^2(7\varphi-10)(\varphi^2-2\varphi+10)^3}\exp\left(\frac{2\big(-2\lambda(\varphi^2-2\varphi+10)+\varphi^2-4\varphi+10\big)}{2\varphi^2-7\varphi+5}\right)\\
&\times\left(2(\varphi-1)^2\big(2\lambda(\varphi^2-2\varphi+10)+2\varphi^2-7\varphi+5\big)e^{\frac{2\lambda(\varphi^2-2\varphi+10)+4\varphi}{2\varphi^2-7\varphi+5}} - \varphi(2\varphi^3 - 9\varphi^2 + 30\varphi - 50)\,e^{\frac{2(\varphi^2+10)}{2\varphi^2-7\varphi+5}}\right),
\end{aligned}
\tag{C13}
$$

$$q_{30} = \Gamma \frac{R^2(13\varphi^5 - 44\varphi^4 + 163\varphi^3 - 310\varphi^2 + 107\varphi - 10)}{648(\varphi-1)^2\varphi^4(7\varphi-10)(5\varphi^2-13\varphi-10)} \exp\left(\frac{2(\lambda(5\varphi^2-13\varphi-10)+(13-6\varphi)\varphi)}{2\varphi^2-7\varphi+5}\right)$$
$$\times\left((1-\varphi)^2(5\varphi^2-13\varphi-10)((6\lambda-1)\varphi+1)e^{\frac{2\lambda(\varphi^2-2\varphi+10)+4\varphi}{2\varphi^2-7\varphi+5}} - 9\,e^{\frac{2(\varphi^2+10)}{2\varphi^2-7\varphi+5}}(5-2\varphi)^2\varphi^3\right). \quad \text{(C14)}$$

They all vanish at high temperature, giving back the well-known Baxter's form for hard spheres.

REFERENCES

[1] J. Hansen and I. McDonald, *Theory of Simple Liquids* (Elsevier Science, 2006), ISBN: 9780080455075, URL: https://books.google.de/books?id=Uhm87WZBnxEC.
[2] W. Götze, *Complex Dynamics of Glass-Forming Liquids* (Oxford University Press, 2008), ISBN: 9780199235346.
[3] M. Sperl, E. Zaccarelli, F. Sciortino, P. Kumar, and H. E. Stanley, Phys. Rev. Lett. **104**, 145701 (2010).
[4] G. Das, N. Gnan, F. Sciortino, and E. Zaccarelli, J. Chem. Phys. **138**, 134501 (2013).
[5] N. Gnan, G. Das, M. Sperl, F. Sciortino, and E. Zaccarelli, Phys. Rev. Lett. **113**, 258302 (2014).
[6] M. S. Wertheim, Phys. Rev. Lett. **10**, 321 (1963).
[7] E. Thiele, J. Chem. Phys. **39**, 3258 (1963).
[8] M. S. Wertheim, J. Math. Phys. **5**, 643 (1964).
[9] R. Baxter, Aust. J. Phys. **21**, 563 (1968).
[10] E. Leutheusser, Physica A **127**, 667 (1984).
[11] S. B. Yuste and A. Santos, Phys. Rev. A **43**, 5418 (1991).
[12] M. S. Ripoll and C. F. Tejero, Mol. Phys. **85**, 423 (1995).
[13] S. B. Yuste, M. L. de Haro, and A. Santos, Phys. Rev. E **53**, 4820 (1996).
[14] M. Robles, M. L. de Haro, and A. Santos, J. Chem. Phys. **120**, 9113 (2004).
[15] M. Robles, M. L. de Haro, and A. Santos, J. Chem. Phys. **125**, 219903(E) (2006).
[16] C. F. Tejero and M. L. de Haro, Mol. Phys. **105**, 2999 (2007).
[17] R. D. Rohrmann and A. Santos, Phys. Rev. E **76**, 051202 (2007).
[18] M. Robles, M. L. de Haro, and A. Santos, J. Chem. Phys. **126**, 016101 (2007).
[19] R. D. Rohrmann, M. Robles, M. L. de Haro, and A. Santos, J. Chem. Phys. **129**, 014510 (2008).
[20] M. Adda-Bedia, E. Katzav, and D. Vella, J. Chem. Phys. **128**, 184508 (2008).
[21] M. Adda-Bedia, E. Katzav, and D. Vella, J. Chem. Phys. **129**, 049901(E) (2008).
[22] M. Adda-Bedia, E. Katzav, and D. Vella, J. Chem. Phys. **129**, 144506 (2008).
[23] E. Katzav, R. Berdichevsky, and M. Schwartz, Phys. Rev. E **99**, 012146 (2019).
[24] S. P. Hlushak, P. A. Hlushak, and A. Trokhymchuk, J. Chem. Phys. **138**, 164107 (2013).
[25] A. Lang, G. Kahl, C. N. Likos, H. Löwen, and M. Watzlawek, J. Phys: Condens. Matter **11**, 10143 (1999).
[26] M. Khanpour and R. Hashim, Phys. Chem. Liq. **51**, 203 (2013).
[27] E.-Y. Kim and S.-C. Kim, J. Korean Phys. Soc. **64**, 844 (2014).
[28] S. B. Yuste, A. Santos, and M. L. de Haro, Mol. Phys. **109**, 987 (2011).
[29] M. L. de Haro, S. B. Yuste, and A. Santos, Mol. Phys. **114**, 2382 (2016).
[30] O. Coquand and M. Sperl, "Temperature expansions in the square shoulder fluid II: Thermodynamics," J. Chem. Phys. (to be published); arXiv:1912.06580 [cond-mat.soft].
[31] K. Dawson, G. Foffi, M. Fuchs, W. Götze, F. Sciortino, M. Sperl, P. Tartaglia, Th. Voigtmann, and E. Zaccarelli, Phys. Rev. E **63**, 011401 (2000).
[32] R. Evans, R. J. F. L. de Carvalho, J. Henderson, and D. Hoyle, J. Chem. Phys. **100**, 591 (1993).
[33] J. Largo and J. R. Solana, Fluid Phase Equilib. **167**, 21 (2000).
[34] A. Trokhymchuk, I. Nezbeda, J. Jirsák, and D. Henderson, J. Chem. Phys. **123**, 024501 (2005).
[35] M. L. de Haro, A. Santos, and S. B. Yuste, J. Chem. Phys. **124**, 236102 (2006).
[36] S. Pieprzyk, A. C. Brańka, and D. M. Heyes, Phys. Rev. E **95**, 062104 (2017).
[37] M. Sperl, Prog. Theor. Phys. Supp. **184**, 211 (2010).
[38] F. J. Rogers and D. A. Young, Phys. Rev. A **30**, 999 (1984).
[39] S. Zhou and J. R. Solana, J. Chem. Phys. **131**, 204503 (2009).
[40] I. Guillén-Escamilla, E. Schöll-Paschinger, and R. Castañeda-Priego, Mol. Phys. **108**, 141 (2010).

[41] Indeed, in most cases, the form of p will depend on T through exponential terms that cannot be Taylor expanded in this regime.